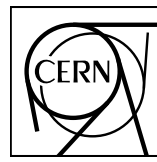


EUROPEAN ORGANIZATION FOR NUCLEAR RESEARCH



CERN-PH-EP-2015-151

17 June 2015

**Centrality dependence of high- p_{T} D meson suppression
in Pb–Pb collisions at $\sqrt{s_{\mathrm{NN}}} = 2.76 \text{ TeV}$**

ALICE Collaboration*

Abstract

The nuclear modification factor, R_{AA} , of the prompt charmed mesons D^0 , D^+ and D^{*+} , and their antiparticles, was measured with the ALICE detector in Pb–Pb collisions at a centre-of-mass energy $\sqrt{s_{\mathrm{NN}}} = 2.76 \text{ TeV}$ in two transverse momentum intervals, $5 < p_{\mathrm{T}} < 8 \text{ GeV}/c$ and $8 < p_{\mathrm{T}} < 16 \text{ GeV}/c$, and in six collision centrality classes. The R_{AA} shows a maximum suppression of a factor of 5–6 in the 10% most central collisions. The suppression and its centrality dependence are compatible within uncertainties with those of charged pions. A comparison with the R_{AA} of non-prompt J/ψ from B meson decays, measured by the CMS Collaboration, hints at a larger suppression of D mesons in the most central collisions.

© 2015 CERN for the benefit of the ALICE Collaboration.

Reproduction of this article or parts of it is allowed as specified in the CC-BY-4.0 license.

*See Appendix A for the list of collaboration members

1 Introduction

When heavy nuclei collide at high energy, a state of strongly-interacting matter with high energy density is expected to form. According to Quantum Chromodynamics (QCD) calculations on the lattice, this state of matter, the so-called Quark-Gluon Plasma (QGP) is characterised by the deconfinement of the colour charge (see e.g. [1–4]). High-momentum partons, produced at the early stage of the nuclear collision, lose energy as they interact with the QGP constituents. This energy loss is expected to proceed via both inelastic (gluon radiation) [5, 6] and elastic (collisional) processes [7–9].

The nuclear modification factor R_{AA} is used to characterise parton energy loss by comparing particle production yields in nucleus–nucleus collisions to a scaled proton–proton (pp) reference, that corresponds to a superposition of independent nucleon–nucleon collisions. R_{AA} is defined as

$$R_{\mathrm{AA}} = \frac{1}{\langle T_{\mathrm{AA}} \rangle} \cdot \frac{dN_{\mathrm{AA}}/dp_{\mathrm{T}}}{d\sigma_{\mathrm{pp}}/dp_{\mathrm{T}}}, \quad (1)$$

where $d\sigma_{\mathrm{pp}}/dp_{\mathrm{T}}$ and $dN_{\mathrm{AA}}/dp_{\mathrm{T}}$ are the transverse momentum (p_{T}) differential cross section and yield in proton–proton and nucleus–nucleus (AA) collisions, respectively. $\langle T_{\mathrm{AA}} \rangle$ is the average nuclear overlap function, estimated within the Glauber model of the nucleus–nucleus collision geometry, and proportional to the average number of nucleon–nucleon (binary) collisions [10, 11]. Energy loss shifts the momentum of quarks and gluons, and thus hadrons, towards lower values, leading to a suppression of hadron yields with respect to binary scaling at p_{T} larger than few GeV/c ($R_{\mathrm{AA}} < 1$).

Energy loss is expected to be smaller for quarks than for gluons because the colour charge factor of quarks is smaller than that of gluons [5, 6]. In the energy regime of the Large Hadron Collider (LHC), light-flavour hadrons with p_{T} ranging from 5 to 20 GeV/c originate predominantly from gluon fragmentation (see e.g. [12]). At variance, charmed mesons provide an experimental tag for a quark parent. Because of their large mass $m_{c,b}$ ($m_c \approx 1.3 \text{ GeV}/c^2$, $m_b \approx 4.5 \text{ GeV}/c^2$ [13]), heavy quarks are produced at the initial stage of heavy-ion collisions in hard scattering processes that are characterised by a timescale $\Delta t < 1/(2m_{c,b}) \sim 0.1(0.01) \text{ fm}/c$ for c (b) quarks. This time is shorter than the formation time of the QGP medium (a recent estimate for the LHC energy is about 0.3 fm/c [14]). As discussed in Ref. [15], this should be the case also for charm and beauty quarks produced in gluon splitting processes, if their transverse momentum is lower than about 50 GeV/c. Therefore, the comparison of the heavy-flavour hadron R_{AA} with that of pions allows the colour-charge dependence of parton energy loss to be tested. The softer fragmentation of gluons than that of charm quarks, and the observed increase of the charged hadron R_{AA} towards high p_{T} [16], tend to counterbalance the effect of the larger energy loss of gluons on the R_{AA} . The model predictions range from a rather moderate effect $R_{\mathrm{AA}}^{\pi} < R_{\mathrm{AA}}^D$ [17–20] to an overall compensation $R_{\mathrm{AA}}^{\pi} \approx R_{\mathrm{AA}}^D$ (as recently shown in [12]) in the p_{T} interval from 5 to about 15 GeV/c.

Several mass-dependent effects are expected to influence the energy loss for quarks (see [15] for a recent review). The dead-cone effect should reduce small-angle gluon radiation for quarks that have moderate energy-over-mass values, i.e. for c and b quarks with momenta up to about 10 and 30 GeV/c, respectively [18, 21–24]. Likewise, collisional energy loss is expected to be reduced for heavier quarks, because the spatial diffusion coefficient that regulates the momentum exchange with the medium is expected to scale as the inverse of the quark mass [25]. In the p_{T} interval up to about 20 GeV/c, where the masses of heavy quarks are not negligible with respect to their momenta, essentially all models predict $R_{\mathrm{AA}}^D < R_{\mathrm{AA}}^B$ [17–20, 26–35], which stems directly from the mass dependence of the quark–medium interaction and is only moderately affected by the different production and fragmentation kinematics of c and b quarks (see e.g. [36]).

A first comparison of light-flavour, charm and beauty hadron nuclear modification factors based on measurements by the ALICE and CMS Collaborations [16, 37, 38] from the 2010 LHC Pb–Pb data at a centre-of-mass energy $\sqrt{s_{\mathrm{NN}}} = 2.76 \text{ TeV}$ was presented in [37]. In this paper we present the centrality

dependence of the D meson R_{AA} in Pb–Pb collisions at the same energy, measured with the ALICE detector [39] using data from both 2010 and 2011 periods (integrated luminosities of about 2.2 and $21 \mu\mathrm{b}^{-1}$, respectively). The focus here is on the study of the parton energy loss; therefore, the data are presented for the high- p_{T} interval $5\text{--}16 \mathrm{GeV}/c$, where the largest suppression relative to binary scaling was observed [37]. The results are compared with charged pions, measured by the ALICE Collaboration [40], with non-prompt J/ψ mesons, measured by the CMS Collaboration [38], and with model predictions.

2 Experimental apparatus and data sample

The Pb–Pb collisions were recorded using a minimum-bias interaction trigger, based on the information of the signal coincidence of the V0 scintillator detectors that cover the full azimuth in the pseudo-rapidity intervals $-3.7 < \eta < -1.7$ and $2.8 < \eta < 5.1$ [41]. The measurement of the summed signal amplitudes from the V0 detectors was used to sort the events in classes of collision centrality, defined in terms of percentiles of the Pb–Pb hadronic cross section [42]. The trigger efficiency is 100% for the events considered in this analysis, which correspond to the most central 80% of the Pb–Pb hadronic cross section. An online selection based on the information of the V0 detectors was applied to increase the statistics of central collisions for the 2011 data sample. An offline selection using the V0 and the neutron Zero-Degree Calorimeters (ZDC) was applied to remove background from interactions of the beams with residual atoms in the vacuum tube. Events with a reconstructed primary vertex outside the interval $\pm 10 \mathrm{cm}$ from the interaction point along the beam direction (z coordinate) were removed. The event sample used in the analysis corresponds to an integrated luminosity $L_{\mathrm{int}} = (21.3 \pm 0.7) \mu\mathrm{b}^{-1}$ in the 0–10% centrality class (16.4×10^6 events) and $(5.8 \pm 0.2) \mu\mathrm{b}^{-1}$ in each of the 10–20%, 20–30%, 30–40%, 40–50% classes (4.5×10^6 events per class). In the 50–80% class, where 2010 data were used, the analyzed event sample corresponds to $(2.2 \pm 0.1) \mu\mathrm{b}^{-1}$ (5.1×10^6 events).

The decays $D^0 \rightarrow K^- \pi^+$, $D^+ \rightarrow K^- \pi^+ \pi^+$ and $D^{*+} \rightarrow D^0 \pi^+$, and their charge conjugates, were reconstructed as described in [37] using the central barrel detectors, which are located in a solenoid that generates a 0.5 T magnetic field parallel to the beam direction. Charged particle tracks were reconstructed with the Time Projection Chamber (TPC) [43] and the Inner Tracking System (ITS), which consists of six cylindrical layers of silicon detectors [44]. Both detectors provide full azimuthal coverage in the interval $|\eta| < 0.9$. D^0 and D^+ candidates were formed from pairs and triplets of tracks with $|\eta| < 0.8$, $p_{\mathrm{T}} > 0.4 \mathrm{GeV}/c$, at least 70 associated space points in the TPC, and at least two hits in the ITS, out of which one had to be in either of the two innermost layers. D^{*+} candidates were formed by combining D^0 candidates with tracks with $|\eta| < 0.8$, $p_{\mathrm{T}} > 0.1 \mathrm{GeV}/c$, and at least three associated hits in the ITS for the 10% most central collisions (two in the other centrality classes). The decay tracks of the candidate D mesons were identified on the basis of their specific ionization energy deposition dE/dx in the TPC and of their flight times to the Time Of Flight (TOF) detector, which has the same η acceptance as the TPC. Particles were identified as pions (kaons) by requiring the measured signal to be within three times the resolution ($\pm 3\sigma$) around the expected mean values of dE/dx and time-of-flight for pions (kaons). Only D meson candidates with rapidity $|y| < 0.8$ were considered, because the acceptance decreases rapidly outside this interval.

3 Data analysis

The selection of the D meson decay topology is mainly based on the displacement of the decay tracks from the primary vertex, and on the pointing of the reconstructed D meson momentum to the primary vertex [37]. The raw yields were determined in each centrality and p_{T} interval using fits to the distributions of invariant mass $M(K^- \pi^+)$ and $M(K^- \pi^+ \pi^+)$, in the case of D^0 and D^+ mesons, and of the difference $M(K^- \pi^+ \pi^+) - M(K^- \pi^+)$ for D^{*+} mesons. The fit function is the sum of a Gaussian, for the signal, and either an exponential function (D^0 and D^+) or a power-law multiplied with an exponential

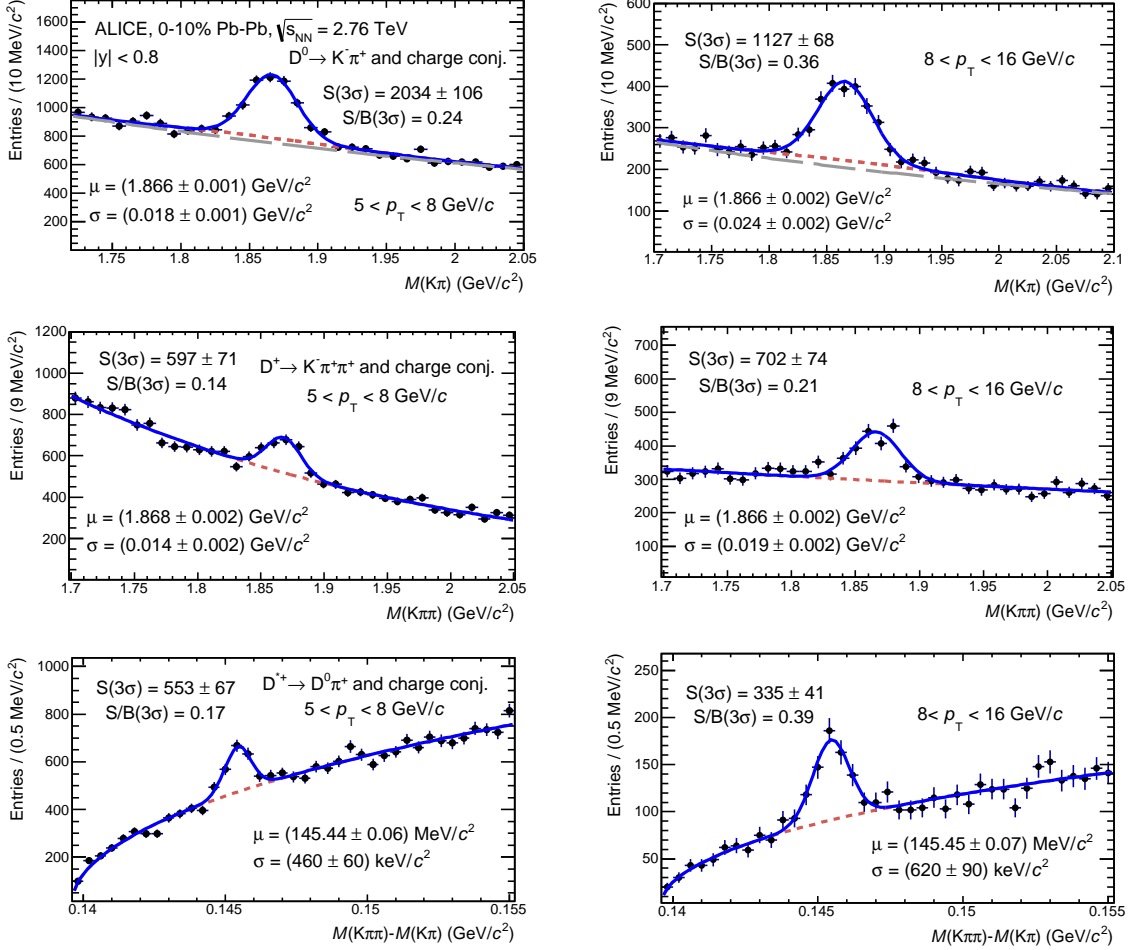


Fig. 1: Distributions of the $K\pi$ invariant mass for D^0 candidates (upper panels) and $K\pi\pi$ invariant mass for D^+ candidates (central panels) and of the invariant mass difference $M(K\pi\pi) - M(K\pi)$ for D^{*+} candidates (lower panels) and the corresponding charge conjugates in two p_T intervals (left and right panels) for 16.4×10^6 Pb–Pb collisions in the 0–10% centrality class. The curves show the fit functions described in the text. The red short-dashed line represents the background fit function. For the D^0 meson, the gray dashed line represents the background without the inclusion of the template for the contribution of reflections, i.e. signal candidates with swapped (K, π) mass hypothesis. The template is defined as the sum of two Gaussians with parameters fixed to the values obtained in simulation.

function (D^{*+}) to describe the background distribution [37].

For D^0 mesons, an additional term was included in the fit function to account for the so-called ‘reflections’, i.e. signal candidates that are present in the invariant mass distribution also when the (K, π) mass hypothesis for the decay tracks is swapped. A large fraction (about 70%) of these reflections is rejected by the particle identification selection. The residual contribution was studied with Monte Carlo simulations (described later in this section). It was found that the reflections have a broad invariant mass distribution, which is well described by a sum of two Gaussians, and its integral amounts to about 30% of the yield of the signal in the p_T interval used in the analysis presented in this article. In order to account for the contribution of reflections in the data, a template consisting of two Gaussians was included in the fit. The centroids and widths, as well as the ratios of the integrals of these Gaussians to the signal integral, were fixed to the values obtained in the simulation (see [45] for more details).

In the most central centrality class (0–10%), the statistical significance of the invariant mass signal peaks varies from 8 to 18 depending on the D meson species and p_T , while the signal-over-background ratio

	$5 < p_{\text{T}} < 8 \text{ GeV}/c$			$8 < p_{\text{T}} < 16 \text{ GeV}/c$		
	D ⁰	D ⁺	D ^{*+}	D ⁰	D ⁺	D ^{*+}
Pb–Pb yields:						
Yield Extraction	6	8	6	7	8	7
Tracking efficiency	10	15	15	10	15	15
PID identification	5	5	5	5	5	5
Cut efficiency	5	10	5	5	10	5
D p_{T} distribution in sim.	2	2	2	2	2	2
Feed-down subtraction	$+12$ -13	$+10$ -10	$+6$ -8	$+12$ -12	$+10$ -10	$+7$ -10
$\langle T_{\text{AA}} \rangle$ [42]		4			4	
pp reference	16	20	17	16	19	17
Reference scaling in \sqrt{s}		$+6$ -12			$+5$ -6	
Centrality limits				< 0.1		

Table 1: Systematic uncertainties (%) on R_{AA} of prompt D mesons with $5 < p_{\text{T}} < 8 \text{ GeV}/c$ and $8 < p_{\text{T}} < 16 \text{ GeV}/c$ in the 0–10% centrality class.

ranges from 0.1 to 0.4. In the most peripheral centrality class (50–80%), the statistical significance varies from 4 to 11, while the signal-over-background ranges from 0.4 to 1.5. In Fig. 1 the invariant mass distributions of the three meson species are shown in the 0–10% centrality class and in the transverse momentum intervals $5 < p_{\text{T}} < 8 \text{ GeV}/c$ and $8 < p_{\text{T}} < 16 \text{ GeV}/c$.

The correction for acceptance and efficiency was determined using Monte Carlo simulations. Pb–Pb events were simulated using the HIJING generator [46] and D meson signals were added with the PYTHIA 6 generator [47]. The p_{T} distribution of the D mesons was weighted in order to match the shape measured for D⁰ mesons in central Pb–Pb collisions [37]. A detailed description of the detector response, based on the GEANT3 transport package [48], was included. The contribution of feed-down from $B \rightarrow D + X$ to the inclusive D meson raw yield depends on p_{T} and on the geometrical selection criteria, because the secondary vertices of D mesons from B-hadron decays are typically more displaced from the primary vertex than those of prompt D mesons. This contribution was subtracted using the beauty-hadron production cross section in pp collisions from FONLL calculations [49], convoluted with the decay kinematics as implemented in the EvtGen decay package [50] and multiplied by the efficiency for feed-down D mesons from the simulation, the average nuclear overlap function $\langle T_{\text{AA}} \rangle$ in each centrality class, and an assumed value for R_{AA} of feed-down D-mesons [37]. On the basis of the comparison shown in this paper, this assumption was taken as $R_{\text{AA}}^{\text{feed-down D}} = 2R_{\text{AA}}^{\text{prompt D}}$ and a systematic uncertainty was estimated by varying it in the interval $1 < R_{\text{AA}}^{\text{feed-down D}}/R_{\text{AA}}^{\text{prompt D}} < 3$. The feed-down contribution is about 20–25%, depending on the D meson species and on the p_{T} interval.

The p_{T} -differential cross section of prompt D mesons with $|y| < 0.5$ in pp collisions at $\sqrt{s} = 2.76 \text{ TeV}$, used as reference for R_{AA} , was obtained by scaling the measurement at $\sqrt{s} = 7 \text{ TeV}$ [51]. The p_{T} -dependent scaling factor and its uncertainty were determined with FONLL calculations [52]. The result of the scaling was validated by comparison with the measurement obtained from a smaller sample of pp collisions at $\sqrt{s} = 2.76 \text{ TeV}$ [53]. This measurement covers a reduced p_{T} interval 1–12 GeV/c with a statistical uncertainty of 20–25 % and was, therefore, not used as a pp reference in the present analysis. The yields in Pb–Pb collisions were normalized to the same rapidity interval as the reference ($|y| < 0.5$) by dividing them by $\Delta y = 1.6$.

The systematic uncertainties were estimated as a function of p_{T} and centrality using the procedure described in [37, 45] and briefly outlined in the following. The sources of systematic uncertainty on the nuclear modification factor are listed in Table 1, along with their values for the two p_{T} intervals in the most central collisions (0–10%). The uncertainties are approximately independent of centrality.

The systematic uncertainty on the yield extraction was estimated by varying the fit conditions (fit interval and functional form used to describe the background) or by considering, as an alternative method, the bin counting of the invariant mass distribution obtained after subtracting the background estimated from a fit in the side-bands of the signal peak. The uncertainty amounts to about 6–8%. This includes in the case of the D^0 a contribution of about 5% obtained by varying the ratio of the integral of the reflections to the integral of the signal by $\pm 50\%$.

The systematic uncertainty on the tracking efficiency correction was evaluated by varying the track selection criteria and amounts to 5% per track, thus 10% for the D^0 (two-track final state) and 15% for the D^+ and D^{*+} mesons (three-track final states). The correction for the particle identification (PID) efficiency introduces a systematic uncertainty of 5%, which was estimated by repeating the analysis without this selection and comparing the corrected yields. A systematic uncertainty of 5–10% associated with the selection efficiency correction was estimated by varying the D meson selection cuts. The D meson p_{T} distribution used in the simulation to calculate the acceptance and efficiency was varied between the measured distribution and the prediction of a theoretical calculation including parton energy loss [32, 54, 55]. The resulting variation of 2% of the efficiencies was assigned as a systematic uncertainty.

The systematic uncertainty on the correction for feed-down from B-hadron decays was estimated, as described in [45], by varying the parameters of the FONLL calculation and the hypothesis on the R_{AA} of the feed-down D mesons in the range $1 < R_{\mathrm{AA}}^{\mathrm{feed-down} \, D} / R_{\mathrm{AA}}^{\mathrm{prompt} \, D} < 3$. This variation yields the main contribution to the uncertainty, which amounts to 6–13%, depending on the D meson species and p_{T} interval.

The contribution to the systematic uncertainty due to the 1.1% relative uncertainty on the fraction of hadronic cross section used in the Glauber fit to determine the centrality classes was obtained as in [37] and estimated to be < 0.1% in the central centrality class (0–10%) and 3% in the most peripheral centrality class (50–80%).

The systematic uncertainties on the denominator of the nuclear modification factor include the uncertainty on $\langle T_{\mathrm{AA}} \rangle$, which ranges from 4% in the 0–10% centrality class to 7.5% in the 50–80% centrality class [42], and the uncertainty on the pp reference. The latter has a contribution of about 16–20% from the pp measurement at $\sqrt{s} = 7 \text{ TeV}$ and a contribution of $^{+12}_{-6}\%$ from the energy scaling down to $\sqrt{s} = 2.76 \text{ TeV}$.

4 Results and discussion

Figure 2 shows the R_{AA} as a function of centrality for D^0 , D^+ and D^{*+} in the intervals $5 < p_{\mathrm{T}} < 8 \text{ GeV}/c$ (left) and $8 < p_{\mathrm{T}} < 16 \text{ GeV}/c$ (right). Centrality is quantified in terms of the average number of nucleons participating in the collision in each multiplicity class, $\langle N_{\mathrm{part}} \rangle$, evaluated with a Monte Carlo Glauber calculation [42]. The bars represent the statistical uncertainties. The filled and empty boxes represent the quadratic sum of the systematic uncertainties that are, respectively, correlated between centrality intervals (pp reference, B-hadron cross section used for feed-down correction, particle identification, track reconstruction efficiency, $\langle T_{\mathrm{AA}} \rangle$) and uncorrelated (yield extraction, selection efficiency corrections, value of feed-down D meson R_{AA}). The latter category also includes the systematic uncertainties that are partially correlated between adjacent centrality classes. The measurements for the three D meson species share part of the systematic uncertainties and are consistent within statistical uncertainties. The suppression increases with centrality and reaches a factor of 5–6 in the most central collisions for both p_{T} intervals.

A weighted average of the R_{AA} of the three D meson species was computed using the inverse of the relative statistical uncertainties as weights. The systematic uncertainties of the weighted average were calculated considering the contributions from the tracking efficiency, the feed-down correction, and the reference energy scaling factor from 7 to 2.76 TeV as fully correlated among the three D meson species.

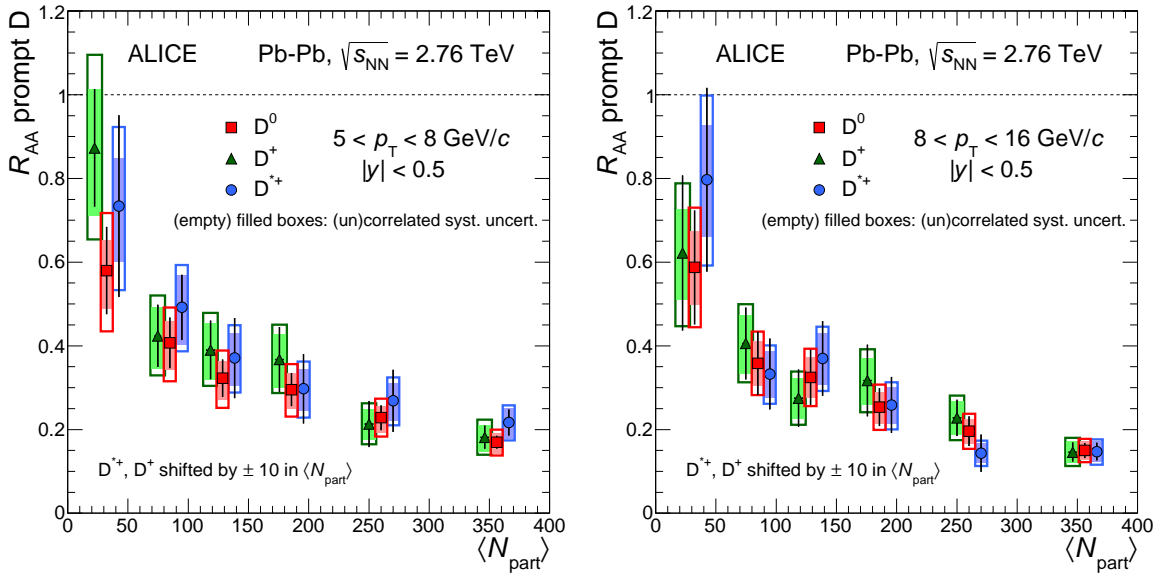


Fig. 2: R_{AA} as a function of centrality ($\langle N_{part} \rangle$, see text) of D^0 , D^+ and D^{*+} in $5 < p_T < 8 \text{ GeV}/c$ (left) and $8 < p_T < 16 \text{ GeV}/c$ (right). The bars represent the statistical uncertainty while the filled (empty) boxes represent the systematic uncertainties that are correlated (uncorrelated) among centrality intervals. The symbols for D^{*+} and D^+ are shifted by $\langle N_{part} \rangle = 10$ for better visibility.

Figure 3 shows the average of the D^0 , D^+ and D^{*+} nuclear modification factors as a function of centrality, for the intervals $5 < p_T < 8 \text{ GeV}/c$ (left) and $8 < p_T < 16 \text{ GeV}/c$ (right), compared with the R_{AA} of charged pions with $|y| < 0.8$ for the same p_T intervals¹, and of non-prompt J/ψ mesons measured by the CMS Collaboration for $6.5 < p_T < 30 \text{ GeV}/c$ in $|y| < 2.4$ [38]. Care has to be taken when comparing with the non-central CMS data point as it is plotted at the N_{part} mean value of the broad 20–100% centrality interval.

The p_T interval 8–16 GeV/c for D mesons was chosen in order to obtain a significant overlap with the p_T distribution of B mesons decaying to J/ψ particles with $6.5 < p_T < 30 \text{ GeV}/c$. Using a simulation based on the FONLL calculation [49] and the EvtGen particle decay package [50], it was estimated that about 70% of these parent B mesons have $8 < p_T < 16 \text{ GeV}/c$, with a median of the p_T distribution of about 11.3 GeV/c . A median value of $(9.5 \pm 0.5) \text{ GeV}/c$ was estimated for D mesons with $8 < p_T < 16 \text{ GeV}/c$ in the 0–10% centrality class. The estimate was based on the p_T distribution of D^0 mesons in p_T intervals with a width of 1 GeV/c . The effect of the different width of the rapidity interval for D and non-prompt J/ψ mesons ($|y| < 0.5$ and $|y| < 2.4$, respectively) is expected to be mild because the intervals are partially overlapping and a preliminary measurement by the CMS Collaboration does not indicate a significant y dependence of the R_{AA} of non-prompt J/ψ mesons in $|y| < 2.4$ [56].

The nuclear modification factors of charged pions and D mesons are compatible within uncertainties in all centrality classes and in the two p_T intervals. The value of the D meson R_{AA} in the centrality classes 0–10% and 10–20% for $8 < p_T < 16 \text{ GeV}/c$ is lower than that of non-prompt J/ψ mesons in the centrality class 0–20%. However, the difference between the R_{AA} values is not larger than 3σ , considering the statistical and systematic uncertainties. A preliminary higher-statistics measurement by the CMS Collaboration of non-prompt J/ψ production in the same p_T interval (6.5–30 GeV/c) and in a narrower rapidity interval ($|y| < 1.2$) is also available [56]. Considering this measurement, the average difference of the R_{AA} values of D mesons and non-prompt J/ψ in the 0–10% and 10–20% centrality classes is larger than zero with a significance of 3.5σ , obtained including the systematic uncertainties, and taking into account their correlation between the two centrality classes.

¹The charged pion results were obtained with the analysis method described in [40].

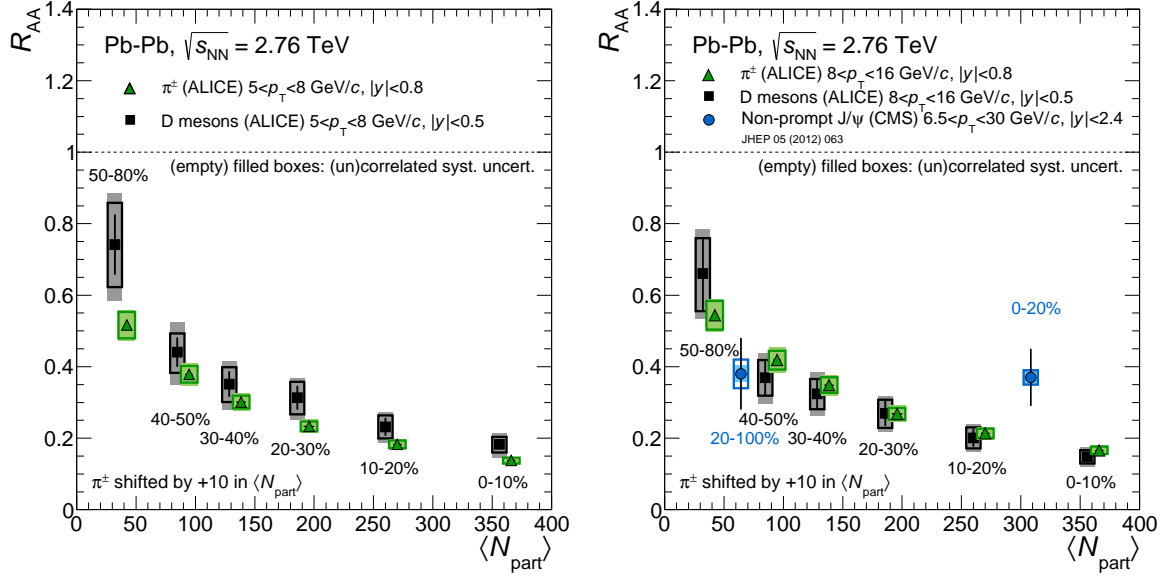


Fig. 3: Comparison of the D meson R_{AA} (average of D^0 , D^+ and D^{*+}) and of the charged pion R_{AA} [40] in $5 < p_T < 8 \text{ GeV}/c$ (left) and in $8 < p_T < 16 \text{ GeV}/c$ (right). The right panel also includes the R_{AA} of non-prompt J/ψ mesons in $6.5 < p_T < 30 \text{ GeV}/c$ measured by the CMS Collaboration [38]. The vertical bars represent the statistical uncertainties. The D meson systematic uncertainties are displayed as in the previous figures. The total systematic uncertainties of charged pions are shown by boxes. The centrality-dependent systematic uncertainties are shown by boxes on the individual data points.

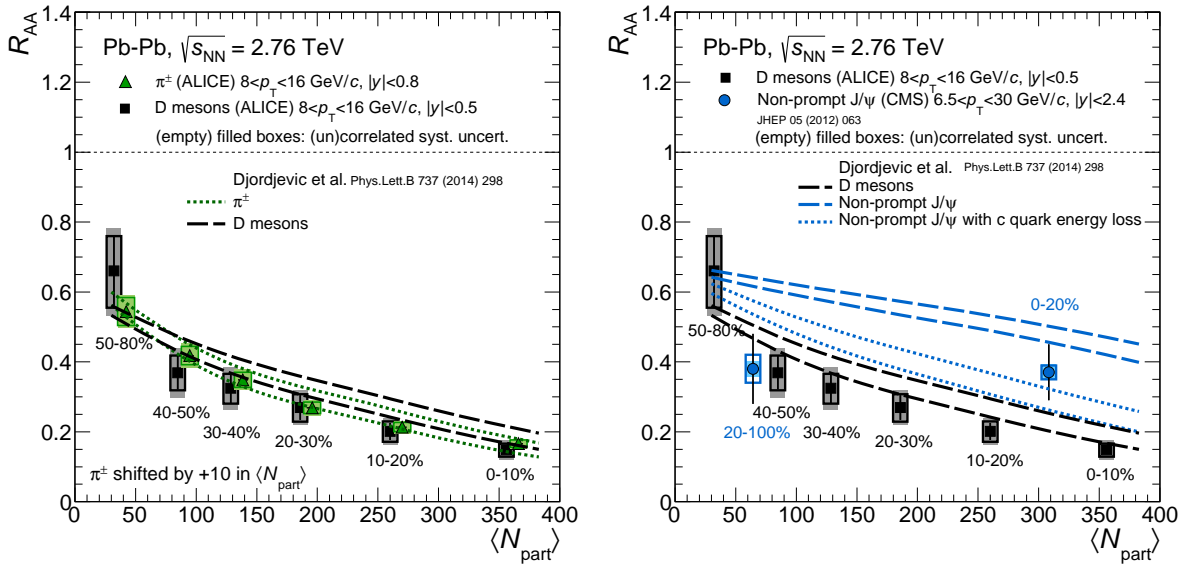


Fig. 4: Comparison of the R_{AA} measurements with the calculations by Djordjevic *et al.* [57] including radiative and collisional energy loss. Lines of the same style enclose a band representing the theoretical uncertainty. Left: D mesons and charged pions in $8 < p_T < 16 \text{ GeV}/c$. Right: D mesons in $8 < p_T < 16 \text{ GeV}/c$ and non-prompt J/ψ mesons in $6.5 < p_T < 30 \text{ GeV}/c$ [38]. For the latter, the model results for the case in which the b quark interactions are calculated using the c quark mass are shown as well [15].

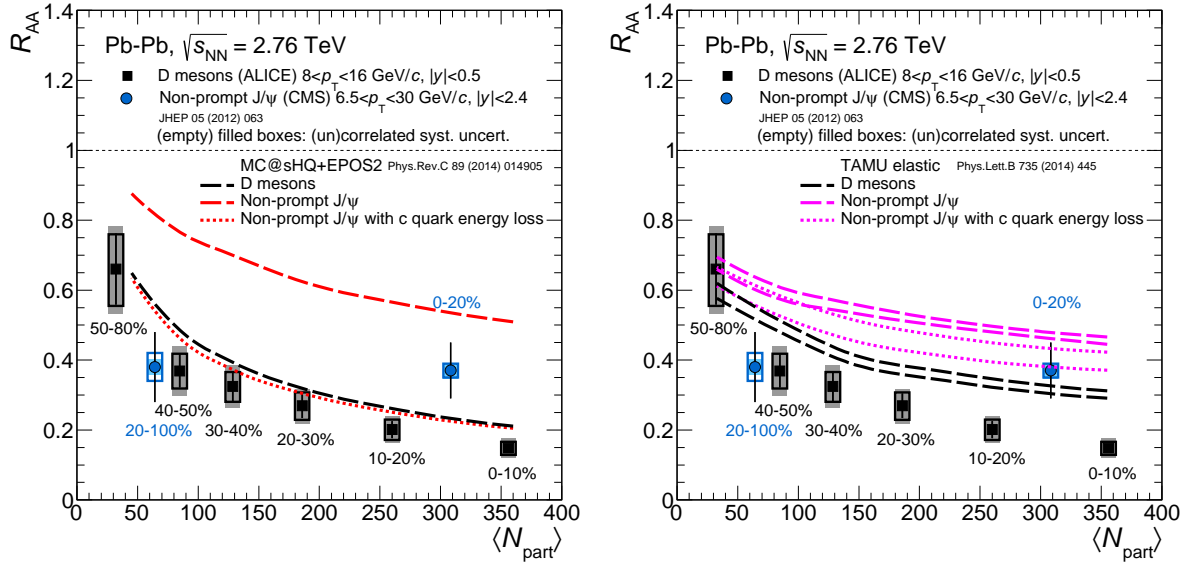


Fig. 5: Comparison of the R_{AA} measurements for D mesons ($8 < p_T < 16 \text{ GeV}/c$) and non-prompt J/ψ mesons ($6.5 < p_T < 30 \text{ GeV}/c$) [38] with the MC@sHQ+EPOS2 model [58] including radiative and collisional interactions (left) and with the TAMU elastic model [29] including collisional interactions via in-medium resonance formation. For both models, results for the case in which the b quark interactions are calculated using the c quark mass are shown as well [15]. In the right-hand panel, the band between lines with the same style represents the theoretical uncertainty.

The nuclear modification factors of D mesons (average of D^0 , D^+ and D^{*+}) and charged pions in the interval $8 < p_T < 16 \text{ GeV}/c$ and that of non-prompt J/ψ mesons in $6.5 < p_T < 30 \text{ GeV}/c$ were compared with theoretical calculations. Figure 4 shows the comparison with the calculation by Djordjevic *et al.* [57]. This model implements energy loss for gluons, light and heavy quarks, including both radiative (DGLV formalism [23]) and collisional processes and considers dynamical scattering centres in the medium. The heavy-quark production p_T -differential cross sections are obtained from FONLL calculations [49] and hadronization assumes fragmentation outside the medium. In the left-hand panel, the calculation closely describes the similarity of the D meson and charged pion R_{AA} over the entire centrality range. As mentioned in the introduction, in this calculation the colour-charge dependence of energy loss introduces a sizeable difference in the suppression of the gluon and c quark production. However, the softer fragmentation and p_T spectrum of gluons with respect to those of c quarks, together with the increase of the parton-level R_{AA} with increasing p_T , lead to a compensation effect that results in a very similar R_{AA} for D mesons and pions [12]. As shown in the right-hand panel of the figure, this calculation results in a larger suppression of D mesons with respect to non-prompt J/ψ , in qualitative agreement with the data for the most central collisions. In order to study the origin of this large difference in the calculation, the result for a test case with the energy loss of b quarks calculated using the c quark mass was considered [15]. In this case, the R_{AA} of non-prompt J/ψ was found to be quite close to that of D mesons. This indicates that, in the calculation, the large difference in the R_{AA} of D mesons and non-prompt J/ψ derives predominantly from the quark mass dependence of the parton energy loss.

In Fig. 5 the D meson and non-prompt J/ψ data are compared with two theoretical models that implement heavy-quark interactions in an expanding hydrodynamical medium. The MC@sHQ+EPOS2 model [58], shown in the left-hand panel, includes radiative and collisional energy loss. The hydrodynamical evolution of the medium is simulated using the EPOS2 model [59, 60]. Heavy-quark transport in the medium is based on the Boltzmann equation, with collisional processes and radiative corrections. The TAMU elastic model [29], shown in the right-hand panel, includes collisional (elastic) processes only. In this model, the heavy-quark transport coefficient is calculated within a non-perturbative T -matrix approach, where

the interactions proceed via resonance formation that transfers momentum from the heavy quarks to the medium constituents. The model includes hydrodynamic medium evolution, constrained by light-flavour hadron production data. Elastic diffusion of heavy-flavour hadrons in the hadronic phase is included as well. In both models, similarly to that of Djordjevic *et al.*, the heavy-quark production cross sections are obtained from the FONLL calculation [49]. Both models implement a contribution of quark recombination in the hadronization of heavy quarks, in addition to fragmentation outside the medium. The dotted lines correspond to the test case in which the b quark mass is decreased to the c quark mass value in the calculation of the in-medium interactions [15].

The MC@shQ+EPOS2 model qualitatively describes the two measurements in these p_{T} intervals. In this model a large difference in the suppression of D mesons and non-prompt J/ ψ is caused by the mass dependence of energy loss as in Djordjevic *et al.* model. The TAMU elastic model tends to overestimate R_{AA} for both the non-prompt J/ ψ and the D mesons, in particular in central collisions. At variance with the other two models, in this case the quark mass effect accounts for only about half of the difference in the suppression of D and non-prompt J/ ψ mesons. This model does not include radiative energy loss, which is expected to have a strong mass dependence.

The nuclear modification factors of D mesons and non-prompt J/ ψ are also described by a model calculation by the Duke group [61], that includes radiative and collisional energy loss within an hydrodynamical medium and performs the hadronization of heavy quarks using recombination and fragmentation.

5 Summary

The centrality dependence of the nuclear modification factor of prompt D mesons in Pb–Pb collisions at $\sqrt{s_{\mathrm{NN}}} = 2.76$ TeV was presented in the intervals $5 < p_{\mathrm{T}} < 8$ GeV/c and $8 < p_{\mathrm{T}} < 16$ GeV/c. A suppression is observed already in the centrality class 50–80% and it increases towards more central collisions, reaching a maximum of a factor about 5–6 in the most central collisions.

The centrality dependence and the magnitude of the suppression are similar to those of charged pions in the same p_{T} intervals. The comparison of the D meson R_{AA} with the non-prompt J/ ψ meson R_{AA} hints at a difference in the suppression of particles originating from c and b quarks in the most central collisions.

These results are described by theoretical calculations in which in-medium parton energy loss increases with increasing colour charge factor and decreases with increasing quark mass. Calculations that include radiative energy loss, in addition to collisional energy loss, provide a better quantitative description of the data.

Acknowledgements

The ALICE Collaboration would like to thank all its engineers and technicians for their invaluable contributions to the construction of the experiment and the CERN accelerator teams for the outstanding performance of the LHC complex. The ALICE Collaboration gratefully acknowledges the resources and support provided by all Grid centres and the Worldwide LHC Computing Grid (WLCG) collaboration. The ALICE Collaboration acknowledges the following funding agencies for their support in building and running the ALICE detector: State Committee of Science, World Federation of Scientists (WFS) and Swiss Fonds Kidagan, Armenia, Conselho Nacional de Desenvolvimento Científico e Tecnológico (CNPq), Financiadora de Estudos e Projetos (FINEP), Fundação de Amparo à Pesquisa do Estado de São Paulo (FAPESP); National Natural Science Foundation of China (NSFC), the Chinese Ministry of Education (CMOE) and the Ministry of Science and Technology of China (MSTC); Ministry of Education and Youth of the Czech Republic; Danish Natural Science Research Council, the Carlsberg Foundation and the Danish National Research Foundation; The European Research Council under the European

Community's Seventh Framework Programme; Helsinki Institute of Physics and the Academy of Finland; French CNRS-IN2P3, the 'Region Pays de Loire', 'Region Alsace', 'Region Auvergne' and CEA, France; German Bundesministerium fur Bildung, Wissenschaft, Forschung und Technologie (BMBF) and the Helmholtz Association; General Secretariat for Research and Technology, Ministry of Development, Greece; Hungarian Orszagos Tudomanyos Kutatasi Alappgrammok (OTKA) and National Office for Research and Technology (NKTH); Department of Atomic Energy and Department of Science and Technology of the Government of India; Istituto Nazionale di Fisica Nucleare (INFN) and Centro Fermi - Museo Storico della Fisica e Centro Studi e Ricerche "Enrico Fermi", Italy; MEXT Grant-in-Aid for Specially Promoted Research, Japan; Joint Institute for Nuclear Research, Dubna; National Research Foundation of Korea (NRF); Consejo Nacional de Ciencia y Tecnologia (CONACYT), Direccion General de Asuntos del Personal Academic(DGAPA), Mexico, Amerique Latine Formation academique - European Commission (ALFA-EC) and the EPLANET Program (European Particle Physics Latin American Network); Stichting voor Fundamenteel Onderzoek der Materie (FOM) and the Nederlandse Organisatie voor Wetenschappelijk Onderzoek (NWO), Netherlands; Research Council of Norway (NFR); National Science Centre, Poland; Ministry of National Education/Institute for Atomic Physics and National Council of Scientific Research in Higher Education (CNCSI-UEFISCDI), Romania; Ministry of Education and Science of Russian Federation, Russian Academy of Sciences, Russian Federal Agency of Atomic Energy, Russian Federal Agency for Science and Innovations and The Russian Foundation for Basic Research; Ministry of Education of Slovakia; Department of Science and Technology, South Africa; Centro de Investigaciones Energeticas, Medioambientales y Tecnologicas (CIEMAT), E-Infrastructure shared between Europe and Latin America (EELA), Ministerio de Economía y Competitividad (MINECO) of Spain, Xunta de Galicia (Consellería de Educación), Centro de Aplicaciones Tecnológicas y Desarrollo Nuclear (CEADEN), Cubaenergía, Cuba, and IAEA (International Atomic Energy Agency); Swedish Research Council (VR) and Knut & Alice Wallenberg Foundation (KAW); Ukraine Ministry of Education and Science; United Kingdom Science and Technology Facilities Council (STFC); The United States Department of Energy, the United States National Science Foundation, the State of Texas, and the State of Ohio; Ministry of Science, Education and Sports of Croatia and Unity through Knowledge Fund, Croatia. Council of Scientific and Industrial Research (CSIR), New Delhi, India

References

- [1] F. Karsch, "Lattice simulations of the thermodynamics of strongly interacting elementary particles and the exploration of new phases of matter in relativistic heavy ion collisions," *J.Phys.Conf.Ser.* **46** (2006) 122–131, [arXiv:hep-lat/0608003 \[hep-lat\]](https://arxiv.org/abs/hep-lat/0608003).
- [2] **Wuppertal-Budapest** Collaboration, S. Borsanyi *et al.*, "Is there still any T_c mystery in lattice QCD? Results with physical masses in the continuum limit III," *JHEP* **1009** (2010) 073, [arXiv:1005.3508 \[hep-lat\]](https://arxiv.org/abs/1005.3508).
- [3] S. Borsanyi, Z. Fodor, C. Hoelbling, S. D. Katz, S. Krieg, *et al.*, "Full result for the QCD equation of state with 2+1 flavors," *Phys.Lett.* **B730** (2014) 99–104, [arXiv:1309.5258 \[hep-lat\]](https://arxiv.org/abs/1309.5258).
- [4] A. Bazavov, T. Bhattacharya, M. Cheng, C. DeTar, H. Ding, *et al.*, "The chiral and deconfinement aspects of the QCD transition," *Phys.Rev.* **D85** (2012) 054503, [arXiv:1111.1710 \[hep-lat\]](https://arxiv.org/abs/1111.1710).
- [5] M. Gyulassy and M. Plumer, "Jet Quenching in Dense Matter," *Phys.Lett.* **B243** (1990) 432–438.
- [6] R. Baier, Y. L. Dokshitzer, A. H. Mueller, S. Peigne, and D. Schiff, "Radiative energy loss and p_T broadening of high-energy partons in nuclei," *Nucl.Phys.* **B484** (1997) 265–282, [arXiv:hep-ph/9608322 \[hep-ph\]](https://arxiv.org/abs/hep-ph/9608322).
- [7] M. H. Thoma and M. Gyulassy, "Quark Damping and Energy Loss in the High Temperature QCD," *Nucl.Phys.* **B351** (1991) 491–506.

- [8] E. Braaten and M. H. Thoma, “Energy loss of a heavy quark in the quark-gluon plasma,” *Phys.Rev.* **D44** (1991) 2625–2630.
- [9] E. Braaten and M. H. Thoma, “Energy loss of a heavy fermion in a hot plasma,” *Phys.Rev.* **D44** (1991) 1298–1310.
- [10] ed. W. E. Brittin *et al.*, “R. J. Glauber in Lectures in Theoretical Physics,” *Interscience Publishers, NY, Vol. 1* (1959) 315.
- [11] M. L. Miller, K. Reygers, S. J. Sanders, and P. Steinberg, “Glauber modeling in high energy nuclear collisions,” *Ann.Rev.Nucl.Part.Sci.* **57** (2007) 205–243, arXiv:nucl-ex/0701025 [nucl-ex].
- [12] M. Djordjevic, “Heavy flavor puzzle at LHC: a serendipitous interplay of jet suppression and fragmentation,” *Phys.Rev.Lett.* **112** no. 4, (2014) 042302, arXiv:1307.4702 [nucl-th].
- [13] **Particle Data Group** Collaboration, J. Beringer *et al.*, “Review of Particle Physics (RPP),” *Phys.Rev.* **D86** (2012) 010001.
- [14] F.-M. Liu and S.-X. Liu, “Quark-gluon plasma formation time and direct photons from heavy ion collisions,” *Phys.Rev.* **C89** no. 3, (2014) 034906, arXiv:1212.6587 [nucl-th].
- [15] A. Andronic, F. Arleo, R. Arnaldi, A. Beraudo, E. Bruna, *et al.*, “Heavy-flavour and quarkonium production in the LHC era: from proton-proton to heavy-ion collisions,” arXiv:1506.03981 [nucl-ex].
- [16] **ALICE** Collaboration, B. Abelev *et al.*, “Centrality Dependence of Charged Particle Production at Large Transverse Momentum in Pb–Pb Collisions at $\sqrt{s_{\text{NN}}} = 2.76 \text{ TeV}$,” *Phys.Lett.* **B720** (2013) 52–62, arXiv:1208.2711 [hep-ex].
- [17] N. Armesto, A. Dainese, C. A. Salgado, and U. A. Wiedemann, “Testing the color charge and mass dependence of parton energy loss with heavy-to-light ratios at RHIC and CERN LHC,” *Phys.Rev.* **D71** ((2005)) 054027, arXiv:hep-ph/0501225 [hep-ph].
- [18] S. Wicks, W. Horowitz, M. Djordjevic, and M. Gyulassy, “Elastic, inelastic, and path length fluctuations in jet tomography,” *Nucl.Phys.* **A784** (2007) 426–442, arXiv:nucl-th/0512076 [nucl-th].
- [19] W. Horowitz and M. Gyulassy, “The Surprising Transparency of the sQGP at LHC,” *Nucl.Phys.* **A872** (2011) 265–285, arXiv:1104.4958 [hep-ph].
- [20] W. Horowitz, “Testing pQCD and AdS/CFT Energy Loss at RHIC and LHC,” *AIP Conf.Proc.* **1441** (2012) 889–891, arXiv:1108.5876 [hep-ph].
- [21] Y. L. Dokshitzer and D. Kharzeev, “Heavy quark colorimetry of QCD matter,” *Phys.Lett.* **B519** (2001) 199–206, arXiv:hep-ph/0106202 [hep-ph].
- [22] N. Armesto, C. A. Salgado, and U. A. Wiedemann, “Medium induced gluon radiation off massive quarks fills the dead cone,” *Phys.Rev.* **D69** (2004) 114003, arXiv:hep-ph/0312106 [hep-ph].
- [23] M. Djordjevic and M. Gyulassy, “Heavy quark radiative energy loss in QCD matter,” *Nucl.Phys.* **A733** (2004) 265–298, arXiv:nucl-th/0310076 [nucl-th].
- [24] B.-W. Zhang, E. Wang, and X.-N. Wang, “Heavy quark energy loss in nuclear medium,” *Phys.Rev.Lett.* **93** (2004) 072301, arXiv:nucl-th/0309040 [nucl-th].

- [25] H. van Hees, V. Greco, and R. Rapp, “Heavy-quark probes of the quark-gluon plasma at RHIC,” *Phys.Rev.* **C73** (2006) 034913, arXiv:nucl-th/0508055 [nucl-th].
- [26] A. Adil and I. Vitev, “Collisional dissociation of heavy mesons in dense QCD matter,” *Phys.Lett.* **B649** (2007) 139–146, arXiv:hep-ph/0611109 [hep-ph].
- [27] R. Sharma, I. Vitev, and B.-W. Zhang, “Light-cone wave function approach to open heavy flavor dynamics in QCD matter,” *Phys.Rev.* **C80** (2009) 054902, arXiv:0904.0032 [hep-ph].
- [28] A. Buzzatti and M. Gyulassy, “A running coupling explanation of the surprising transparency of the QGP at LHC,” *Nucl.Phys.* **A904-905** (2013) 779c–782c, arXiv:1210.6417 [hep-ph].
- [29] M. He, R. J. Fries, and R. Rapp, “Non-perturbative Heavy-Flavor Transport at RHIC and LHC,” *Nucl.Phys.* **A910-911** (2013) 409–412, arXiv:1208.0256 [nucl-th].
- [30] M. He, R. J. Fries, and R. Rapp, “Heavy Flavor at the Large Hadron Collider in a Strong Coupling Approach,” *Phys.Lett.* **B735** (2014) 445–450, arXiv:1401.3817 [nucl-th].
- [31] P. Gossiaux, M. Nahrgang, M. Bluhm, T. Gousset, and J. Aichelin, “Heavy quark quenching from RHIC to LHC and the consequences of gluon damping,” *Nucl.Phys.* **A904-905** (2013) 992c–995c, arXiv:1211.2281 [hep-ph].
- [32] J. Uphoff, O. Fochler, Z. Xu, and C. Greiner, “Open Heavy Flavor in Pb+Pb Collisions at $\sqrt{s} = 2.76$ TeV within a Transport Model,” *Phys.Lett.* **B717** (2012) 430–435, arXiv:1205.4945 [hep-ph].
- [33] W. Alberico, A. Beraudo, A. De Pace, A. Molinari, M. Monteno, *et al.*, “Heavy flavors in AA collisions: production, transport and final spectra,” *Eur.Phys.J.* **C73** (2013) 2481, arXiv:1305.7421 [hep-ph].
- [34] S. Cao, G.-Y. Qin, and S. A. Bass, “Heavy-quark dynamics and hadronization in ultrarelativistic heavy-ion collisions: Collisional versus radiative energy loss,” *Phys.Rev.* **C88** no. 4, (2013) 044907, arXiv:1308.0617 [nucl-th].
- [35] T. Lang, H. van Hees, J. Steinheimer, and M. Bleicher, “Heavy quark transport in heavy ion collisions at RHIC and LHC within the UrQMD transport model,” (2012) 20, arXiv:1211.6912 [hep-ph].
- [36] N. Armesto, N. Borghini, S. Jeon, U. Wiedemann, S. Abreu, *et al.*, “Heavy Ion Collisions at the LHC - Last Call for Predictions,” *J.Phys.* **G35** (2008) 054001, arXiv:0711.0974 [hep-ph].
- [37] **ALICE** Collaboration, B. Abelev *et al.*, “Suppression of high transverse momentum D mesons in central Pb-Pb collisions at $\sqrt{s_{NN}} = 2.76$ TeV,” *JHEP* **1209** (2012) 112, arXiv:1203.2160 [nucl-ex].
- [38] **CMS** Collaboration, S. Chatrchyan *et al.*, “Suppression of non-prompt J/ψ , prompt J/ψ , and $Y(1S)$ in PbPb collisions at $\sqrt{s_{NN}} = 2.76$ TeV,” *JHEP* **1205** (2012) 063, arXiv:1201.5069 [nucl-ex].
- [39] **ALICE** Collaboration, K. Aamodt *et al.*, “The ALICE experiment at the CERN LHC,” *JINST* **3** (2008) S08002.
- [40] **ALICE** Collaboration, B. B. Abelev *et al.*, “Production of charged pions, kaons and protons at large transverse momenta in pp and PbPb collisions at $\sqrt{s_{NN}} = 2.76$ TeV,” *Phys.Lett.* **B736** (2014) 196–207, arXiv:1401.1250 [nucl-ex].

- [41] ALICE Collaboration, E. Abbas *et al.*, “Performance of the ALICE VZERO system,” *JINST* **8** (2013) P10016, arXiv:1306.3130 [nucl-ex].
- [42] ALICE Collaboration, B. Abelev *et al.*, “Centrality determination of Pb-Pb collisions at $\sqrt{s_{\text{NN}}} = 2.76$ TeV with ALICE,” *Phys.Rev.* **C88** no. 4, (2013) 044909, arXiv:1301.4361 [nucl-ex].
- [43] J. Alme, Y. Andres, H. Appelshauser, S. Bablok, N. Bialas, *et al.*, “The ALICE TPC, a large 3-dimensional tracking device with fast readout for ultra-high multiplicity events,” *Nucl.Instrum.Meth.* **A622** (2010) 316–367, arXiv:1001.1950 [physics.ins-det].
- [44] ALICE Collaboration, K. Aamodt *et al.*, “Alignment of the ALICE Inner Tracking System with cosmic-ray tracks,” *JINST* **5** (2010) P03003, arXiv:1001.0502 [physics.ins-det].
- [45] ALICE Collaboration, B. B. Abelev *et al.*, “Azimuthal anisotropy of D meson production in Pb-Pb collisions at $\sqrt{s_{\text{NN}}} = 2.76$ TeV,” *Phys.Rev.* **C90** no. 3, (2014) 034904, arXiv:1405.2001 [nucl-ex].
- [46] X.-N. Wang and M. Gyulassy, “HIJING: A Monte Carlo model for multiple jet production in p-p, p-A and A-A collisions,” *Phys.Rev.* **D44** (1991) 3501–3516.
- [47] T. Sjostrand, S. Mrenna, and P. Z. Skands, “PYTHIA 6.4 Physics and Manual,” *JHEP* **0605** (2006) 026, arXiv:hep-ph/0603175 [hep-ph].
- [48] R. Brun, F. Carminati, and S. Giani, “GEANT Detector Description and Simulation Tool,” *CERN-W5013, CERN-W-5013* (1994) .
- [49] M. Cacciari, S. Frixione, N. Houdeau, M. L. Mangano, P. Nason, *et al.*, “Theoretical predictions for charm and bottom production at the LHC,” *JHEP* **1210** (2012) 137, arXiv:1205.6344 [hep-ph].
- [50] D. Lange, “The EvtGen particle decay simulation package,” *Nucl.Instrum.Meth.* **A462** (2001) 152–155.
- [51] ALICE Collaboration, B. Abelev *et al.*, “Measurement of charm production at central rapidity in proton-proton collisions at $\sqrt{s} = 7$ TeV,” *JHEP* **1201** (2012) 128, arXiv:1111.1553 [hep-ex].
- [52] R. Averbeck, N. Bastid, Z. C. del Valle, P. Crochet, A. Dainese, *et al.*, “Reference Heavy Flavour Cross Sections in pp Collisions at $\sqrt{s} = 2.76$ TeV, using a pQCD-Driven \sqrt{s} – Scaling of ALICE Measurements at $\sqrt{s} = 7$ TeV,” arXiv:1107.3243 [hep-ph].
- [53] ALICE Collaboration, B. Abelev *et al.*, “Measurement of charm production at central rapidity in proton-proton collisions at $\sqrt{s} = 2.76$ TeV,” *JHEP* **1207** (2012) 191, arXiv:1205.4007 [hep-ex].
- [54] J. Uphoff, O. Fochler, Z. Xu, and C. Greiner, “Elliptic Flow and Energy Loss of Heavy Quarks in Ultra-Relativistic heavy Ion Collisions,” *Phys.Rev.* **C84** (2011) 024908, arXiv:1104.2295 [hep-ph].
- [55] O. Fochler, J. Uphoff, Z. Xu, and C. Greiner, “Jet quenching and elliptic flow at RHIC and LHC within a pQCD-based partonic transport model,” *J.Phys.* **G38** (2011) 124152, arXiv:1107.0130 [hep-ph].
- [56] CMS Collaboration, C. Collaboration, “ J/ψ results from CMS in PbPb collisions, with $150 \mu b^{-1}$ data,” *CMS-PAS-HIN-12-014* (2012) .

- [57] M. Djordjevic, M. Djordjevic, and B. Blagojevic, “RHIC and LHC jet suppression in non-central collisions,” *Phys.Lett.* **B737** (2014) 298–302, arXiv:1405.4250 [nucl-th].
- [58] M. Nahrgang, J. Aichelin, P. B. Gossiaux, and K. Werner, “Influence of hadronic bound states above T_c on heavy-quark observables in Pb+Pb collisions at the CERN Large Hadron Collider,” *Phys.Rev.* **C89** no. 1, (2014) 014905, arXiv:1305.6544 [hep-ph].
- [59] K. Werner, I. Karpenko, T. Pierog, M. Bleicher, and K. Mikhailov, “Event-by-Event Simulation of the Three-Dimensional Hydrodynamic Evolution from Flux Tube Initial Conditions in Ultrarelativistic Heavy Ion Collisions,” *Phys.Rev.* **C82** (2010) 044904, arXiv:1004.0805 [nucl-th].
- [60] K. Werner, I. Karpenko, M. Bleicher, T. Pierog, and S. Porteboeuf-Houssais, “Jets, Bulk Matter, and their Interaction in Heavy Ion Collisions at Several TeV,” *Phys.Rev.* **C85** (2012) 064907, arXiv:1203.5704 [nucl-th].
- [61] S. Cao, G.-Y. Qin, and S. A. Bass, “Energy loss, hadronization and hadronic interactions of heavy flavors in relativistic heavy-ion collisions,” arXiv:1505.01413 [nucl-th].

A ALICE Collaboration

J. Adam⁴⁰, D. Adamová⁸³, M.M. Aggarwal⁸⁷, G. Aglieri Rinella³⁶, M. Agnello¹¹¹, N. Agrawal⁴⁸, Z. Ahammed¹³², S.U. Ahn⁶⁸, I. Aimo^{94,111}, S. Aiola¹³⁷, M. Ajaz¹⁶, A. Akindinov⁵⁸, S.N. Alam¹³², D. Aleksandrov¹⁰⁰, B. Alessandro¹¹¹, D. Alexandre¹⁰², R. Alfaro Molina⁶⁴, A. Alici^{105,12}, A. Alkin³, J.R.M. Almaraz¹¹⁹, J. Alme³⁸, T. Alt⁴³, S. Altinpinar¹⁸, I. Altsybeev¹³¹, C. Alves Garcia Prado¹²⁰, C. Andrei⁷⁸, A. Andronic⁹⁷, V. Anguelov⁹³, J. Anielski⁵⁴, T. Antičić⁹⁸, F. Antinori¹⁰⁸, P. Antonioli¹⁰⁵, L. Aphecetche¹¹³, H. Appelhäuser⁵³, S. Arcelli²⁸, N. Armesto¹⁷, R. Arnaldi¹¹¹, I.C. Arsene²², M. Arslanbekov⁵³, B. Audurier¹¹³, A. Augustinus³⁶, R. Averbeck⁹⁷, M.D. Azmi¹⁹, M. Bach⁴³, A. Badalà¹⁰⁷, Y.W. Baek⁴⁴, S. Bagnasco¹¹¹, R. Bailhache⁵³, R. Bala⁹⁰, A. Baldissari¹⁵, F. Baltasar Dos Santos Pedrosa³⁶, R.C. Baral⁶¹, A.M. Barbano¹¹¹, R. Barbera²⁹, F. Barile³³, G.G. Barnaföldi¹³⁶, L.S. Barnby¹⁰², V. Barret⁷⁰, P. Bartalini⁷, K. Barth³⁶, J. Bartke¹¹⁷, E. Bartsch⁵³, M. Basile²⁸, N. Bastid⁷⁰, S. Basu¹³², B. Bathen⁵⁴, G. Batigne¹¹³, A. Batista Camejo⁷⁰, B. Batyunya⁶⁶, P.C. Batzing²², I.G. Bearden⁸⁰, H. Beck⁵³, C. Bedda¹¹¹, N.K. Behera^{48,49}, I. Belikov⁵⁵, F. Bellini²⁸, H. Bello Martinez², R. Bellwied¹²², R. Belmont¹³⁵, E. Belmont-Moreno⁶⁴, V. Belyaev⁷⁶, G. Bencedi¹³⁶, S. Beole²⁷, I. Berceanu⁷⁸, A. Bercuci⁷⁸, Y. Berdnikov⁸⁵, D. Berenyi¹³⁶, R.A. Bertens⁵⁷, D. Berzana^{36,27}, L. Betev³⁶, A. Bhasin⁹⁰, I.R. Bhat⁹⁰, A.K. Bhati⁸⁷, B. Bhattacharjee⁴⁵, J. Bhom¹²⁸, L. Bianchi¹²², N. Bianchi⁷², C. Bianchin^{135,57}, J. Bielčík⁴⁰, J. Bielčíková⁸³, A. Bilandžić⁸⁰, R. Biswas⁴, S. Biswas⁷⁹, S. Bjelogrlic⁵⁷, F. Blanco¹⁰, D. Blau¹⁰⁰, C. Blume⁵³, F. Bock^{74,93}, A. Bogdanov⁷⁶, H. Bøggild⁸⁰, L. Boldizsár¹³⁶, M. Bombara⁴¹, J. Book⁵³, H. Borel¹⁵, A. Borissov⁹⁶, M. Borri⁸², F. Bossú⁶⁵, E. Botta²⁷, S. Böttger⁵², P. Braun-Munzinger⁹⁷, M. Bregant¹²⁰, T. Breitner⁵², T.A. Broker⁵³, T.A. Browning⁹⁵, M. Broz⁴⁰, E.J. Brucken⁴⁶, E. Bruna¹¹¹, G.E. Bruno³³, D. Budnikov⁹⁹, H. Buesching⁵³, S. Bufalino^{36,111}, P. Buncic³⁶, O. Busch^{93,128}, Z. Buthelezi⁶⁵, J.B. Butt¹⁶, J.T. Buxton²⁰, D. Caffarri³⁶, X. Cai⁷, H. Caines¹³⁷, L. Calero Diaz⁷², A. Caliva⁵⁷, E. Calvo Villar¹⁰³, P. Camerini²⁶, F. Carena³⁶, W. Carena³⁶, J. Castillo Castellanos¹⁵, A.J. Castro¹²⁵, E.A.R. Casula²⁵, C. Cavicchioli³⁶, C. Ceballos Sanchez⁹, J. Cepila⁴⁰, P. Cerello¹¹¹, J. Cerkala¹¹⁵, B. Chang¹²³, S. Chapeland³⁶, M. Chartier¹²⁴, J.L. Charvet¹⁵, S. Chattopadhyay¹³², S. Chattopadhyay¹⁰¹, V. Chelnokov³, M. Cherney⁸⁶, C. Cheshkov¹³⁰, B. Cheynis¹³⁰, V. Chibante Barroso³⁶, D.D. Chinellato¹²¹, P. Chochula³⁶, K. Choi⁹⁶, M. Chojnacki⁸⁰, S. Choudhury¹³², P. Christakoglou⁸¹, C.H. Christensen⁸⁰, P. Christiansen³⁴, T. Chujo¹²⁸, S.U. Chung⁹⁶, Z. Chunhui⁵⁷, C. Cicalo¹⁰⁶, L. Cifarelli^{12,28}, F. Cindolo¹⁰⁵, J. Cleymans⁸⁹, F. Colamaria³³, D. Colella^{36,59,33}, A. Collu²⁵, M. Colocci²⁸, G. Conesa Balbastre⁷¹, Z. Conesa del Valle⁵¹, M.E. Connors¹³⁷, J.G. Contreras^{11,40}, T.M. Cormier⁸⁴, Y. Corrales Morales²⁷, I. Cortés Maldonado², P. Cortese³², M.R. Cosentino¹²⁰, F. Costa³⁶, P. Crochet⁷⁰, R. Cruz Albino¹¹, E. Cuautle⁶³, L. Cunqueiro³⁶, T. Dahms^{92,37}, A. Dainese¹⁰⁸, A. Danu⁶², D. Das¹⁰¹, I. Das^{51,101}, S. Das⁴, A. Dash¹²¹, S. Dash⁴⁸, S. De¹²⁰, A. De Caro^{31,12}, G. de Cataldo¹⁰⁴, J. de Cuveland⁴³, A. De Falco²⁵, D. De Gruttola^{12,31}, N. De Marco¹¹¹, S. De Pasquale³¹, A. Deisting^{97,93}, A. Deloff⁷⁷, E. Dénes¹³⁶, G. D'Erasmo³³, D. Di Bari³³, A. Di Mauro³⁶, P. Di Nezza⁷², M.A. Diaz Corchero¹⁰, T. Dietel⁸⁹, P. Dillenseger⁵³, R. Divià³⁶, Ø. Djupsland¹⁸, A. Dobrin^{57,81}, T. Dobrowolski^{77,1}, D. Domenicis Gimenez¹²⁰, B. Dönigus⁵³, O. Dordic²², A.K. Dubey¹³², A. Dubla⁵⁷, L. Ducroux¹³⁰, P. Dupieux⁷⁰, R.J. Ehlers¹³⁷, D. Elia¹⁰⁴, H. Engel⁵², B. Erazmus^{36,113}, I. Erdemir⁵³, F. Erhardt¹²⁹, D. Eschweiler⁴³, B. Espagnon⁵¹, M. Estienne¹¹³, S. Esumi¹²⁸, J. Eum⁹⁶, D. Evans¹⁰², S. Evdokimov¹¹², G. Eyyubova⁴⁰, L. Fabbietti^{37,92}, D. Fabris¹⁰⁸, J. Faivre⁷¹, A. Fantoni⁷², M. Fasel⁷⁴, L. Feldkamp⁵⁴, D. Felea⁶², A. Feliciello¹¹¹, G. Feofilov¹³¹, J. Ferencei⁸³, A. Fernández Téllez², E.G. Ferreiro¹⁷, A. Ferretti²⁷, A. Festanti³⁰, V.J.G. Feuillard^{15,70}, J. Figiel¹¹⁷, M.A.S. Figueiredo¹²⁴, S. Filchagin⁹⁹, D. Finogeev⁵⁶, E.M. Fiore³³, M.G. Fleck⁹³, M. Floris³⁶, S. Foertsch⁶⁵, P. Foka⁹⁷, S. Fokin¹⁰⁰, E. Fragiocomo¹¹⁰, A. Francescon^{30,36}, U. Frankenfeld⁹⁷, U. Fuchs³⁶, C. Furget⁷¹, A. Furs⁵⁶, M. Fusco Girard³¹, J.J. Gaardhøje⁸⁰, M. Gagliardi²⁷, A.M. Gago¹⁰³, M. Gallio²⁷, D.R. Gangadharan⁷⁴, P. Ganoti⁸⁸, C. Gao⁷, C. Garabatos⁹⁷, E. Garcia-Solis¹³, C. Gargiulo³⁶, P. Gasik^{92,37}, M. Germain¹¹³, A. Gheata³⁶, M. Gheata^{62,36}, P. Ghosh¹³², S.K. Ghosh⁴, P. Gianotti⁷², P. Giubellino^{36,111}, P. Giubilato³⁰, E. Gladysz-Dziadus¹¹⁷, P. Glässel⁹³, A. Gomez Ramirez⁵², P. González-Zamora¹⁰, S. Gorbunov⁴³, L. Görlich¹¹⁷, S. Gotovac¹¹⁶, V. Grabski⁶⁴, L.K. Graczykowski¹³⁴, K.L. Graham¹⁰², A. Grelli⁵⁷, A. Grigoras³⁶, C. Grigoras³⁶, V. Grigoriev⁷⁶, A. Grigoryan¹, S. Grigoryan⁶⁶, B. Grinyov³, N. Grion¹¹⁰, J.F. Grosse-Oetringhaus³⁶, J.-Y. Grossiord¹³⁰, R. Grossiord³⁶, F. Guber⁵⁶, R. Guernane⁷¹, B. Guerzoni²⁸, K. Gulbrandsen⁸⁰, H. Gulkanyan¹, T. Gunji¹²⁷, A. Gupta⁹⁰, R. Gupta⁹⁰, R. Haake⁵⁴, Ø. Haaland¹⁸, C. Hadjidakis⁵¹, M. Haiduc⁶², H. Hamagaki¹²⁷, G. Hamar¹³⁶, A. Hansen⁸⁰, J.W. Harris¹³⁷, H. Hartmann⁴³, A. Harton¹³, D. Hatzifotiadou¹⁰⁵, S. Hayashi¹²⁷, S.T. Heckel⁵³, M. Heide⁵⁴, H. Helstrup³⁸, A. Herghelegiu⁷⁸, G. Herrera Corral¹¹, B.A. Hess³⁵, K.F. Hetland³⁸, T.E. Hilden⁴⁶, H. Hillemanns³⁶, B. Hippolyte⁵⁵, R. Hosokawa¹²⁸, P. Hristov³⁶, M. Huang¹⁸, T.J. Humanic²⁰, N. Hussain⁴⁵, T. Hussain¹⁹, D. Hutter⁴³, D.S. Hwang²¹, R. Ilkaev⁹⁹, I. Ilkiv⁷⁷, M. Inaba¹²⁸, M. Ippolitov^{76,100}, M. Irfan¹⁹, M. Ivanov⁹⁷, V. Ivanov⁸⁵, V. Izucheev¹¹², P.M. Jacobs⁷⁴, S. Jadlovska¹¹⁵,

C. Jahnke¹²⁰, H.J. Jang⁶⁸, M.A. Janik¹³⁴, P.H.S.Y. Jayarathna¹²², C. Jena³⁰, S. Jena¹²², R.T. Jimenez Bustamante⁹⁷, P.G. Jones¹⁰², H. Jung⁴⁴, A. Jusko¹⁰², P. Kalinak⁵⁹, A. Kalweit³⁶, J. Kamin⁵³, J.H. Kang¹³⁸, V. Kaplin⁷⁶, S. Kar¹³², A. Karasu Uysal⁶⁹, O. Karavichev⁵⁶, T. Karavicheva⁵⁶, L. Karayan^{97,93}, E. Karpechev⁵⁶, U. Kebschull⁵², R. Keidel¹³⁹, D.L.D. Keijdener⁵⁷, M. Keil³⁶, K.H. Khan¹⁶, M.M. Khan¹⁹, P. Khan¹⁰¹, S.A. Khan¹³², A. Khanzadeev⁸⁵, Y. Kharlov¹¹², B. Kileng³⁸, B. Kim¹³⁸, D.W. Kim^{44,68}, D.J. Kim¹²³, H. Kim¹³⁸, J.S. Kim⁴⁴, M. Kim⁴⁴, M. Kim¹³⁸, S. Kim²¹, T. Kim¹³⁸, S. Kirsch⁴³, I. Kisel⁴³, S. Kiselev⁵⁸, A. Kisiel¹³⁴, G. Kiss¹³⁶, J.L. Klay⁶, C. Klein⁵³, J. Klein^{36,93}, C. Klein-Bösing⁵⁴, A. Kluge³⁶, M.L. Knichel⁹³, A.G. Knospe¹¹⁸, T. Kobayashi¹²⁸, C. Kobdaj¹¹⁴, M. Kofarago³⁶, T. Kollegger^{97,43}, A. Kolojvari¹³¹, V. Kondratiev¹³¹, N. Kondratyeva⁷⁶, E. Kondratyuk¹¹², A. Konevskikh⁵⁶, M. Kopcik¹¹⁵, M. Kour⁹⁰, C. Kouzinopoulos³⁶, O. Kovalenko⁷⁷, V. Kovalenko¹³¹, M. Kowalski¹¹⁷, G. Koyithatta Meethaleveedu⁴⁸, J. Kral¹²³, I. Králik⁵⁹, A. Kravčáková⁴¹, M. Krelina⁴⁰, M. Kretz⁴³, M. Krivda^{102,59}, F. Krizek⁸³, E. Kryshen³⁶, M. Krzewicki⁴³, A.M. Kubera²⁰, V. Kučera⁸³, T. Kugathasan³⁶, C. Kuhn⁵⁵, P.G. Kuijer⁸¹, I. Kulakov⁴³, A. Kumar⁹⁰, J. Kumar⁴⁸, L. Kumar^{79,87}, P. Kurashvili⁷⁷, A. Kurepin⁵⁶, A.B. Kurepin⁵⁶, A. Kuryakin⁹⁹, S. Kushpil⁸³, M.J. Kweon⁵⁰, Y. Kwon¹³⁸, S.L. La Pointe¹¹¹, P. La Rocca²⁹, C. Lagana Fernandes¹²⁰, I. Lakomov³⁶, R. Langoy⁴², C. Lara⁵², A. Lardeux¹⁵, A. Lattuca²⁷, E. Laudi³⁶, R. Lea²⁶, L. Leardini⁹³, G.R. Lee¹⁰², S. Lee¹³⁸, I. Legrand³⁶, F. Lehas⁸¹, R.C. Lemmon⁸², V. Lenti¹⁰⁴, E. Leogrande⁵⁷, I. León Monzón¹¹⁹, M. Leoncino²⁷, P. Léval¹³⁶, S. Li^{7,70}, X. Li¹⁴, J. Lien⁴², R. Lietava¹⁰², S. Lindal²², V. Lindenstruth⁴³, C. Lippmann⁹⁷, M.A. Lisa²⁰, H.M. Ljunggren³⁴, D.F. Lodato⁵⁷, P.I. Loenne¹⁸, V. Loginov⁷⁶, C. Loizides⁷⁴, X. Lopez⁷⁰, E. López Torres⁹, A. Lowe¹³⁶, P. Luettig⁵³, M. Lunardon³⁰, G. Luparello²⁶, P.H.F.N.D. Luz¹²⁰, A. Maevskaia⁵⁶, M. Mager³⁶, S. Mahajan⁹⁰, S.M. Mahmood²², A. Maire⁵⁵, R.D. Majka¹³⁷, M. Malaev⁸⁵, I. Maldonado Cervantes⁶³, L. Malinina^{ii,66}, D. Mal'Kevich⁵⁸, P. Malzacher⁹⁷, A. Mamontov⁹⁹, V. Manko¹⁰⁰, F. Manso⁷⁰, V. Manzari^{36,104}, M. Marchisone²⁷, J. Mareš⁶⁰, G.V. Margagliotti²⁶, A. Margotti¹⁰⁵, J. Margutti⁵⁷, A. Marín⁹⁷, C. Markert¹¹⁸, M. Marquard⁵³, N.A. Martin⁹⁷, J. Martin Blanco¹¹³, P. Martinengo³⁶, M.I. Martínez², G. Martínez García¹¹³, M. Martinez Pedreira³⁶, Y. Martynov³, A. Mas¹²⁰, S. Masciocchi⁹⁷, M. Masera²⁷, A. Masoni¹⁰⁶, L. Massacrier¹¹³, A. Mastroserio³³, H. Masui¹²⁸, A. Matyja¹¹⁷, C. Mayer¹¹⁷, J. Mazer¹²⁵, M.A. Mazzoni¹⁰⁹, D. McDonald¹²², F. Meddi²⁴, Y. Melikyan⁷⁶, A. Menchaca-Rocha⁶⁴, E. Meninno³¹, J. Mercado Pérez⁹³, M. Meres³⁹, Y. Miake¹²⁸, M.M. Mieskolainen⁴⁶, K. Mikhaylov^{58,66}, L. Milano³⁶, J. Milosevic^{22,133}, L.M. Minervini^{104,23}, A. Mischke⁵⁷, A.N. Mishra⁴⁹, D. Miśkowiec⁹⁷, J. Mitra¹³², C.M. Mitu⁶², N. Mohammadi⁵⁷, B. Mohanty^{132,79}, L. Molnar⁵⁵, L. Montaño Zetina¹¹, E. Montes¹⁰, M. Morando³⁰, D.A. Moreira De Godoy^{113,54}, S. Moretto³⁰, A. Morreale¹¹³, A. Morsch³⁶, V. Muccifora⁷², E. Mudnic¹¹⁶, D. Mühlheim⁵⁴, S. Muñuri¹³², M. Mukherjee¹³², J.D. Mulligan¹³⁷, M.G. Munhoz¹²⁰, S. Murray⁶⁵, L. Musa³⁶, J. Musinsky⁵⁹, B.K. Nandi⁴⁸, R. Nania¹⁰⁵, E. Nappi¹⁰⁴, M.U. Naru¹⁶, C. Nattrass¹²⁵, K. Nayak⁷⁹, T.K. Nayak¹³², S. Nazarenko⁹⁹, A. Nedosekin⁵⁸, L. Nellen⁶³, F. Ng¹²², M. Nicassio⁹⁷, M. Niculescu^{62,36}, J. Niedziela³⁶, B.S. Nielsen⁸⁰, S. Nikolaev¹⁰⁰, S. Nikulin¹⁰⁰, V. Nikulin⁸⁵, F. Noferini^{105,12}, P. Nomokonov⁶⁶, G. Nooren⁵⁷, J.C.C. Noris², J. Norman¹²⁴, A. Nyanin¹⁰⁰, J. Nystrand¹⁸, H. Oeschler⁹³, S. Oh¹³⁷, S.K. Oh⁶⁷, A. Ohlson³⁶, A. Okatan⁶⁹, T. Okubo⁴⁷, L. Olah¹³⁶, J. Oleniacz¹³⁴, A.C. Oliveira Da Silva¹²⁰, M.H. Oliver¹³⁷, J. Onderwaater⁹⁷, C. Oppedisano¹¹¹, R. Orava⁴⁶, A. Ortiz Velasquez⁶³, A. Oskarsson³⁴, J. Otwinowski¹¹⁷, K. Oyama⁹³, M. Ozdemir⁵³, Y. Pachmayer⁹³, P. Pagano³¹, G. Paić⁶³, C. Pajares¹⁷, S.K. Pal¹³², J. Pan¹³⁵, A.K. Pandey⁴⁸, D. Pant⁴⁸, P. Papcun¹¹⁵, V. Papikyan¹, G.S. Pappalardo¹⁰⁷, P. Pareek⁴⁹, W.J. Park⁹⁷, S. Parmar⁸⁷, A. Passfeld⁵⁴, V. Paticchio¹⁰⁴, R.N. Patra¹³², B. Paul¹⁰¹, T. Peitzmann⁵⁷, H. Pereira Da Costa¹⁵, E. Pereira De Oliveira Filho¹²⁰, D. Peresunko^{100,76}, C.E. Pérez Lara⁸¹, E. Perez Lezama⁵³, V. Peskov⁵³, Y. Pestov⁵, V. Petráček⁴⁰, V. Petrov¹¹², M. Petrovici⁷⁸, C. Petta²⁹, S. Piano¹¹⁰, M. Píkna³⁹, P. Pillot¹¹³, O. Pinazza^{105,36}, L. Pinsky¹²², D.B. Piyarathna¹²², M. Płoskoń⁷⁴, M. Planinic¹²⁹, J. Pluta¹³⁴, S. Pochybova¹³⁶, P.L.M. Podesta-Lerma¹¹⁹, M.G. Poghosyan^{84,86}, B. Polichtchouk¹¹², N. Poljak¹²⁹, W. Poonsawat¹¹⁴, A. Pop⁷⁸, S. Porteboeuf-Houssais⁷⁰, J. Porter⁷⁴, J. Pospisil⁸³, S.K. Prasad⁴, R. Preghenella^{105,36}, F. Prino¹¹¹, C.A. Pruneau¹³⁵, I. Pshenichnov⁵⁶, M. Puccio¹¹¹, G. Puddu²⁵, P. Pujahari¹³⁵, V. Punin⁹⁹, J. Putschke¹³⁵, H. Qvigstad²², A. Rachevski¹¹⁰, S. Raha⁴, S. Rajput⁹⁰, J. Rak¹²³, A. Rakotozafindrabe¹⁵, L. Ramello³², R. Raniwala⁹¹, S. Raniwala⁹¹, S.S. Räsänen⁴⁶, B.T. Rascanu⁵³, D. Rathee⁸⁷, K.F. Read¹²⁵, J.S. Real⁷¹, K. Redlich⁷⁷, R.J. Reed¹³⁵, A. Rehman¹⁸, P. Reichelt⁵³, F. Reidt^{93,36}, X. Ren⁷, R. Renfordt⁵³, A.R. Reolon⁷², A. Reshetin⁵⁶, F. Rettig⁴³, J.-P. Revol¹², K. Reygers⁹³, V. Riabov⁸⁵, R.A. Ricci⁷³, T. Richert³⁴, M. Richter²², P. Riedler³⁶, W. Riegler³⁶, F. Riggi²⁹, C. Ristea⁶², A. Rivetti¹¹¹, E. Rocco⁵⁷, M. Rodríguez Cahuantzi², A. Rodriguez Manso⁸¹, K. Røed²², E. Rogochaya⁶⁶, D. Rohr⁴³, D. Röhrich¹⁸, R. Romita¹²⁴, F. Ronchetti⁷², L. Ronflette¹¹³, P. Rosnet⁷⁰, A. Rossi^{30,36}, F. Roukoutakis⁸⁸, A. Roy⁴⁹, C. Roy⁵⁵, P. Roy¹⁰¹, A.J. Rubio Montero¹⁰, R. Rui²⁶, R. Russo²⁷, E. Ryabinkin¹⁰⁰, Y. Ryabov⁸⁵, A. Rybicki¹¹⁷, S. Sadovsky¹¹², K. Šafařík³⁶, B. Sahlmuller⁵³, P. Sahoo⁴⁹, R. Sahoo⁴⁹, S. Sahoo⁶¹, P.K. Sahu⁶¹, J. Saini¹³², S. Sakai⁷², M.A. Saleh¹³⁵,

C.A. Salgado¹⁷, J. Salzwedel²⁰, S. Sambyal⁹⁰, V. Samsonov⁸⁵, X. Sanchez Castro⁵⁵, L. Šándor⁵⁹, A. Sandoval⁶⁴, M. Sano¹²⁸, D. Sarkar¹³², E. Scapparone¹⁰⁵, F. Scarlassara³⁰, R.P. Scharenberg⁹⁵, C. Schiaua⁷⁸, R. Schicker⁹³, C. Schmidt⁹⁷, H.R. Schmidt³⁵, S. Schuchmann⁵³, J. Schukraft³⁶, M. Schulc⁴⁰, T. Schuster¹³⁷, Y. Schutz^{113,36}, K. Schwarz⁹⁷, K. Schweda⁹⁷, G. Scioli²⁸, E. Scomparin¹¹¹, R. Scott¹²⁵, K.S. Seeder¹²⁰, J.E. Seger⁸⁶, Y. Sekiguchi¹²⁷, D. Sekihata⁴⁷, I. Selyuzhenkov⁹⁷, K. Senosi⁶⁵, J. Seo^{96,67}, E. Serradilla^{64,10}, A. Sevcenco⁶², A. Shabanov⁵⁶, A. Shabetai¹¹³, O. Shadura³, R. Shahoyan³⁶, A. Shangaraev¹¹², A. Sharma⁹⁰, M. Sharma⁹⁰, M. Sharma⁹⁰, N. Sharma^{125,61}, K. Shigaki⁴⁷, K. Shtejer^{9,27}, Y. Sibiriak¹⁰⁰, S. Siddhanta¹⁰⁶, K.M. Sielewicz³⁶, T. Siemianczuk⁷⁷, D. Silvermyr^{84,34}, C. Silvestre⁷¹, G. Simatovic¹²⁹, G. Simonetti³⁶, R. Singaraju¹³², R. Singh⁷⁹, S. Singha^{132,79}, V. Singhal¹³², B.C. Sinha¹³², T. Sinha¹⁰¹, B. Sitar³⁹, M. Sitta³², T.B. Skaali²², M. Slupecki¹²³, N. Smirnov¹³⁷, R.J.M. Snellings⁵⁷, T.W. Snellman¹²³, C. Søgaard³⁴, R. Soltz⁷⁵, J. Song⁹⁶, M. Song¹³⁸, Z. Song⁷, F. Soramel³⁰, S. Sorensen¹²⁵, M. Spacek⁴⁰, E. Spiriti⁷², I. Sputowska¹¹⁷, M. Spyropoulou-Stassinaki⁸⁸, B.K. Srivastava⁹⁵, J. Stachel⁹³, I. Stan⁶², G. Stefanek⁷⁷, M. Steinpreis²⁰, E. Stenlund³⁴, G. Steyn⁶⁵, J.H. Stiller⁹³, D. Stocco¹¹³, P. Strmen³⁹, A.A.P. Suaide¹²⁰, T. Sugitate⁴⁷, C. Suire⁵¹, M. Suleymanov¹⁶, R. Sultanov⁵⁸, M. Šumbera⁸³, T.J.M. Symons⁷⁴, A. Szabo³⁹, A. Szanto de Toledo^{120,i}, I. Szarka³⁹, A. Szczepankiewicz³⁶, M. Szymanski¹³⁴, J. Takahashi¹²¹, N. Tanaka¹²⁸, M.A. Tangaro³³, J.D. Tapia Takaki^{iii,51}, A. Tarantola Peloni⁵³, M. Tarhini⁵¹, M. Tariq¹⁹, M.G. Tarzila⁷⁸, A. Tauro³⁶, G. Tejeda Muñoz², A. Telesca³⁶, K. Terasaki¹²⁷, C. Terrevoli^{30,25}, B. Teyssier¹³⁰, J. Thäder^{74,97}, D. Thomas¹¹⁸, R. Tieulent¹³⁰, A.R. Timmins¹²², A. Toia⁵³, S. Trogolo¹¹¹, V. Trubnikov³, W.H. Trzaska¹²³, T. Tsuji¹²⁷, A. Tumkin⁹⁹, R. Turrisi¹⁰⁸, T.S. Tveter²², K. Ullaland¹⁸, A. Uras¹³⁰, G.L. Usai²⁵, A. Utrobicic¹²⁹, M. Vajzer⁸³, M. Vala⁵⁹, L. Valencia Palomo⁷⁰, S. Vallero²⁷, J. Van Der Maarel⁵⁷, J.W. Van Hoorn³⁶, M. van Leeuwen⁵⁷, T. Vanat⁸³, P. Vande Vyvre³⁶, D. Varga¹³⁶, A. Vargas², M. Vargyas¹²³, R. Varma⁴⁸, M. Vasileiou⁸⁸, A. Vasiliev¹⁰⁰, A. Vauthier⁷¹, V. Vechernin¹³¹, A.M. Veen⁵⁷, M. Veldhoen⁵⁷, A. Velure¹⁸, M. Venaruzzo⁷³, E. Vercellin²⁷, S. Vergara Limón², R. Vernet⁸, M. Verweij^{135,36}, L. Vickovic¹¹⁶, G. Viesti^{30,i}, J. Viinikainen¹²³, Z. Vilakazi¹²⁶, O. Villalobos Baillie¹⁰², A. Vinogradov¹⁰⁰, L. Vinogradov¹³¹, Y. Vinogradov^{99,i}, T. Virgili³¹, V. Vislavicius³⁴, Y.P. Viyogi¹³², A. Vodopyanov⁶⁶, M.A. Völkl⁹³, K. Voloshin⁵⁸, S.A. Voloshin¹³⁵, G. Volpe^{136,36}, B. von Haller³⁶, I. Vorobyev^{37,92}, D. Vranic^{36,97}, J. Vrláková⁴¹, B. Vulpescu⁷⁰, A. Vyushin⁹⁹, B. Wagner¹⁸, J. Wagner⁹⁷, H. Wang⁵⁷, M. Wang^{7,113}, Y. Wang⁹³, D. Watanabe¹²⁸, Y. Watanabe¹²⁷, M. Weber³⁶, S.G. Weber⁹⁷, J.P. Wessels⁵⁴, U. Westerhoff⁵⁴, J. Wiechula³⁵, J. Wikne²², M. Wilde⁵⁴, G. Wilk⁷⁷, J. Wilkinson⁹³, M.C.S. Williams¹⁰⁵, B. Windelband⁹³, M. Winn⁹³, C.G. Yaldo¹³⁵, H. Yang⁵⁷, P. Yang⁷, S. Yano⁴⁷, Z. Yin⁷, H. Yokoyama¹²⁸, I.-K. Yoo⁹⁶, V. Yurchenko³, I. Yushmanov¹⁰⁰, A. Zaborowska¹³⁴, V. Zaccolo⁸⁰, A. Zaman¹⁶, C. Zampolli¹⁰⁵, H.J.C. Zanolli¹²⁰, S. Zaporozhets⁶⁶, N. Zardoshti¹⁰², A. Zarochentsev¹³¹, P. Závada⁶⁰, N. Zaviyalov⁹⁹, H. Zbroszczyk¹³⁴, I.S. Zgura⁶², M. Zhalov⁸⁵, H. Zhang^{18,7}, X. Zhang⁷⁴, Y. Zhang⁷, C. Zhao²², N. Zhigareva⁵⁸, D. Zhou⁷, Y. Zhou^{80,57}, Z. Zhou¹⁸, H. Zhu^{18,7}, J. Zhu^{113,7}, X. Zhu⁷, A. Zichichi^{12,28}, A. Zimmermann⁹³, M.B. Zimmermann^{54,36}, G. Zinovjev³, M. Zyzak⁴³

Affiliation notes

ⁱ Deceased

ⁱⁱ Also at: M.V. Lomonosov Moscow State University, D.V. Skobeltsyn Institute of Nuclear Physics, Moscow, Russia

ⁱⁱⁱ Also at: University of Kansas, Lawrence, Kansas, United States

Collaboration Institutes

¹ A.I. Alikhanyan National Science Laboratory (Yerevan Physics Institute) Foundation, Yerevan, Armenia

² Benemérita Universidad Autónoma de Puebla, Puebla, Mexico

³ Bogolyubov Institute for Theoretical Physics, Kiev, Ukraine

⁴ Bose Institute, Department of Physics and Centre for Astroparticle Physics and Space Science (CAPSS), Kolkata, India

⁵ Budker Institute for Nuclear Physics, Novosibirsk, Russia

⁶ California Polytechnic State University, San Luis Obispo, California, United States

⁷ Central China Normal University, Wuhan, China

⁸ Centre de Calcul de l'IN2P3, Villeurbanne, France

⁹ Centro de Aplicaciones Tecnológicas y Desarrollo Nuclear (CEADEN), Havana, Cuba

¹⁰ Centro de Investigaciones Energéticas Medioambientales y Tecnológicas (CIEMAT), Madrid, Spain

¹¹ Centro de Investigación y de Estudios Avanzados (CINVESTAV), Mexico City and Mérida, Mexico

- ¹² Centro Fermi - Museo Storico della Fisica e Centro Studi e Ricerche “Enrico Fermi”, Rome, Italy
¹³ Chicago State University, Chicago, Illinois, USA
¹⁴ China Institute of Atomic Energy, Beijing, China
¹⁵ Commissariat à l’Energie Atomique, IRFU, Saclay, France
¹⁶ COMSATS Institute of Information Technology (CIIT), Islamabad, Pakistan
¹⁷ Departamento de Física de Partículas and IGFAE, Universidad de Santiago de Compostela, Santiago de Compostela, Spain
¹⁸ Department of Physics and Technology, University of Bergen, Bergen, Norway
¹⁹ Department of Physics, Aligarh Muslim University, Aligarh, India
²⁰ Department of Physics, Ohio State University, Columbus, Ohio, United States
²¹ Department of Physics, Sejong University, Seoul, South Korea
²² Department of Physics, University of Oslo, Oslo, Norway
²³ Dipartimento di Elettrotecnica ed Elettronica del Politecnico, Bari, Italy
²⁴ Dipartimento di Fisica dell’Università ‘La Sapienza’ and Sezione INFN Rome, Italy
²⁵ Dipartimento di Fisica dell’Università and Sezione INFN, Cagliari, Italy
²⁶ Dipartimento di Fisica dell’Università and Sezione INFN, Trieste, Italy
²⁷ Dipartimento di Fisica dell’Università and Sezione INFN, Turin, Italy
²⁸ Dipartimento di Fisica e Astronomia dell’Università and Sezione INFN, Bologna, Italy
²⁹ Dipartimento di Fisica e Astronomia dell’Università and Sezione INFN, Catania, Italy
³⁰ Dipartimento di Fisica e Astronomia dell’Università and Sezione INFN, Padova, Italy
³¹ Dipartimento di Fisica ‘E.R. Caianiello’ dell’Università and Gruppo Collegato INFN, Salerno, Italy
³² Dipartimento di Scienze e Innovazione Tecnologica dell’Università del Piemonte Orientale and Gruppo Collegato INFN, Alessandria, Italy
³³ Dipartimento Interateneo di Fisica ‘M. Merlin’ and Sezione INFN, Bari, Italy
³⁴ Division of Experimental High Energy Physics, University of Lund, Lund, Sweden
³⁵ Eberhard Karls Universität Tübingen, Tübingen, Germany
³⁶ European Organization for Nuclear Research (CERN), Geneva, Switzerland
³⁷ Excellence Cluster Universe, Technische Universität München, Munich, Germany
³⁸ Faculty of Engineering, Bergen University College, Bergen, Norway
³⁹ Faculty of Mathematics, Physics and Informatics, Comenius University, Bratislava, Slovakia
⁴⁰ Faculty of Nuclear Sciences and Physical Engineering, Czech Technical University in Prague, Prague, Czech Republic
⁴¹ Faculty of Science, P.J. Šafárik University, Košice, Slovakia
⁴² Faculty of Technology, Buskerud and Vestfold University College, Vestfold, Norway
⁴³ Frankfurt Institute for Advanced Studies, Johann Wolfgang Goethe-Universität Frankfurt, Frankfurt, Germany
⁴⁴ Gangneung-Wonju National University, Gangneung, South Korea
⁴⁵ Gauhati University, Department of Physics, Guwahati, India
⁴⁶ Helsinki Institute of Physics (HIP), Helsinki, Finland
⁴⁷ Hiroshima University, Hiroshima, Japan
⁴⁸ Indian Institute of Technology Bombay (IIT), Mumbai, India
⁴⁹ Indian Institute of Technology Indore, Indore (IITI), India
⁵⁰ Inha University, Incheon, South Korea
⁵¹ Institut de Physique Nucléaire d’Orsay (IPNO), Université Paris-Sud, CNRS-IN2P3, Orsay, France
⁵² Institut für Informatik, Johann Wolfgang Goethe-Universität Frankfurt, Frankfurt, Germany
⁵³ Institut für Kernphysik, Johann Wolfgang Goethe-Universität Frankfurt, Frankfurt, Germany
⁵⁴ Institut für Kernphysik, Westfälische Wilhelms-Universität Münster, Münster, Germany
⁵⁵ Institut Pluridisciplinaire Hubert Curien (IPHC), Université de Strasbourg, CNRS-IN2P3, Strasbourg, France
⁵⁶ Institute for Nuclear Research, Academy of Sciences, Moscow, Russia
⁵⁷ Institute for Subatomic Physics of Utrecht University, Utrecht, Netherlands
⁵⁸ Institute for Theoretical and Experimental Physics, Moscow, Russia
⁵⁹ Institute of Experimental Physics, Slovak Academy of Sciences, Košice, Slovakia
⁶⁰ Institute of Physics, Academy of Sciences of the Czech Republic, Prague, Czech Republic
⁶¹ Institute of Physics, Bhubaneswar, India
⁶² Institute of Space Science (ISS), Bucharest, Romania

- ⁶³ Instituto de Ciencias Nucleares, Universidad Nacional Autónoma de México, Mexico City, Mexico
⁶⁴ Instituto de Física, Universidad Nacional Autónoma de México, Mexico City, Mexico
⁶⁵ iThemba LABS, National Research Foundation, Somerset West, South Africa
⁶⁶ Joint Institute for Nuclear Research (JINR), Dubna, Russia
⁶⁷ Konkuk University, Seoul, South Korea
⁶⁸ Korea Institute of Science and Technology Information, Daejeon, South Korea
⁶⁹ KTO Karatay University, Konya, Turkey
⁷⁰ Laboratoire de Physique Corpusculaire (LPC), Clermont Université, Université Blaise Pascal, CNRS-IN2P3, Clermont-Ferrand, France
⁷¹ Laboratoire de Physique Subatomique et de Cosmologie, Université Grenoble-Alpes, CNRS-IN2P3, Grenoble, France
⁷² Laboratori Nazionali di Frascati, INFN, Frascati, Italy
⁷³ Laboratori Nazionali di Legnaro, INFN, Legnaro, Italy
⁷⁴ Lawrence Berkeley National Laboratory, Berkeley, California, United States
⁷⁵ Lawrence Livermore National Laboratory, Livermore, California, United States
⁷⁶ Moscow Engineering Physics Institute, Moscow, Russia
⁷⁷ National Centre for Nuclear Studies, Warsaw, Poland
⁷⁸ National Institute for Physics and Nuclear Engineering, Bucharest, Romania
⁷⁹ National Institute of Science Education and Research, Bhubaneswar, India
⁸⁰ Niels Bohr Institute, University of Copenhagen, Copenhagen, Denmark
⁸¹ Nikhef, Nationaal instituut voor subatomaire fysica, Amsterdam, Netherlands
⁸² Nuclear Physics Group, STFC Daresbury Laboratory, Daresbury, United Kingdom
⁸³ Nuclear Physics Institute, Academy of Sciences of the Czech Republic, Řež u Prahy, Czech Republic
⁸⁴ Oak Ridge National Laboratory, Oak Ridge, Tennessee, United States
⁸⁵ Petersburg Nuclear Physics Institute, Gatchina, Russia
⁸⁶ Physics Department, Creighton University, Omaha, Nebraska, United States
⁸⁷ Physics Department, Panjab University, Chandigarh, India
⁸⁸ Physics Department, University of Athens, Athens, Greece
⁸⁹ Physics Department, University of Cape Town, Cape Town, South Africa
⁹⁰ Physics Department, University of Jammu, Jammu, India
⁹¹ Physics Department, University of Rajasthan, Jaipur, India
⁹² Physik Department, Technische Universität München, Munich, Germany
⁹³ Physikalisches Institut, Ruprecht-Karls-Universität Heidelberg, Heidelberg, Germany
⁹⁴ Politecnico di Torino, Turin, Italy
⁹⁵ Purdue University, West Lafayette, Indiana, United States
⁹⁶ Pusan National University, Pusan, South Korea
⁹⁷ Research Division and ExtreMe Matter Institute EMMI, GSI Helmholtzzentrum für Schwerionenforschung, Darmstadt, Germany
⁹⁸ Rudjer Bošković Institute, Zagreb, Croatia
⁹⁹ Russian Federal Nuclear Center (VNIIEF), Sarov, Russia
¹⁰⁰ Russian Research Centre Kurchatov Institute, Moscow, Russia
¹⁰¹ Saha Institute of Nuclear Physics, Kolkata, India
¹⁰² School of Physics and Astronomy, University of Birmingham, Birmingham, United Kingdom
¹⁰³ Sección Física, Departamento de Ciencias, Pontificia Universidad Católica del Perú, Lima, Peru
¹⁰⁴ Sezione INFN, Bari, Italy
¹⁰⁵ Sezione INFN, Bologna, Italy
¹⁰⁶ Sezione INFN, Cagliari, Italy
¹⁰⁷ Sezione INFN, Catania, Italy
¹⁰⁸ Sezione INFN, Padova, Italy
¹⁰⁹ Sezione INFN, Rome, Italy
¹¹⁰ Sezione INFN, Trieste, Italy
¹¹¹ Sezione INFN, Turin, Italy
¹¹² SSC IHEP of NRC Kurchatov institute, Protvino, Russia
¹¹³ SUBATECH, Ecole des Mines de Nantes, Université de Nantes, CNRS-IN2P3, Nantes, France
¹¹⁴ Suranaree University of Technology, Nakhon Ratchasima, Thailand
¹¹⁵ Technical University of Košice, Košice, Slovakia

- ¹¹⁶ Technical University of Split FESB, Split, Croatia
¹¹⁷ The Henryk Niewodniczanski Institute of Nuclear Physics, Polish Academy of Sciences, Cracow, Poland
¹¹⁸ The University of Texas at Austin, Physics Department, Austin, Texas, USA
¹¹⁹ Universidad Autónoma de Sinaloa, Culiacán, Mexico
¹²⁰ Universidade de São Paulo (USP), São Paulo, Brazil
¹²¹ Universidade Estadual de Campinas (UNICAMP), Campinas, Brazil
¹²² University of Houston, Houston, Texas, United States
¹²³ University of Jyväskylä, Jyväskylä, Finland
¹²⁴ University of Liverpool, Liverpool, United Kingdom
¹²⁵ University of Tennessee, Knoxville, Tennessee, United States
¹²⁶ University of the Witwatersrand, Johannesburg, South Africa
¹²⁷ University of Tokyo, Tokyo, Japan
¹²⁸ University of Tsukuba, Tsukuba, Japan
¹²⁹ University of Zagreb, Zagreb, Croatia
¹³⁰ Université de Lyon, Université Lyon 1, CNRS/IN2P3, IPN-Lyon, Villeurbanne, France
¹³¹ V. Fock Institute for Physics, St. Petersburg State University, St. Petersburg, Russia
¹³² Variable Energy Cyclotron Centre, Kolkata, India
¹³³ Vinča Institute of Nuclear Sciences, Belgrade, Serbia
¹³⁴ Warsaw University of Technology, Warsaw, Poland
¹³⁵ Wayne State University, Detroit, Michigan, United States
¹³⁶ Wigner Research Centre for Physics, Hungarian Academy of Sciences, Budapest, Hungary
¹³⁷ Yale University, New Haven, Connecticut, United States
¹³⁸ Yonsei University, Seoul, South Korea
¹³⁹ Zentrum für Technologietransfer und Telekommunikation (ZTT), Fachhochschule Worms, Worms, Germany